



Impact of increased resolution on long-standing biases in HighResMIP-PRIMAVERA climate models

Eduardo Moreno-Chamarro^{1*}, Louis-Philippe Caron^{1,2}, Saskia Loosveldt Tomas¹, Oliver Gutjahr^{3,4}, Marie-Pierre Moine⁵, Dian Putrasahan³, Christopher D. Roberts⁶, Malcolm J. Roberts⁷, Retish Senan⁶,
5 Laurent Terray⁵, Etienne Tourigny¹, Pier Luigi Vidale⁸

¹ Barcelona Supercomputing Center (BSC), Barcelona, Spain.

² Now at Ouranos, Montreal, H3A 1B9, Canada.

³ Max Planck Institute for Meteorology, Hamburg, Germany.

⁴ Now at Institut für Meereskunde, Universität Hamburg, Hamburg, Germany.

10 ⁵ CECI, Université de Toulouse, CERFACS/CNRS, Toulouse, France.

⁶ ECMWF European Centre for Medium-Range Weather Forecasts, Reading, United Kingdom.

⁷ Met Office, Exeter EX1 3PB, United Kingdom.

⁸ NCAS-Climate, Department of Meteorology, University of Reading, Reading, United Kingdom.

Correspondence to: Eduardo Moreno-Chamarro (eduardo.moreno@bsc.es)

15 **Abstract.** We examine the impacts of increased resolution on four long-standing biases using five different climate models developed within the PRIMAVERA project. Atmospheric resolution is increased from $\sim 100\text{--}200$ km to $\sim 25\text{--}50$ km, and ocean resolution is increased from $\sim 1^\circ$ (i.e., eddy-parametrized) to $\sim 0.25^\circ$ (i.e., eddy-present). For one model, ocean resolution is also increased to $1/12^\circ$ (i.e., eddy-rich). Fully-coupled general circulation models and their atmosphere-only versions are compared with observations and reanalysis of near-surface temperature, precipitation, cloud cover, net cloud
20 radiative effect, and zonal wind over the period 1980–2014. Both the ensemble mean and individual models are analyzed. Increased resolution especially in the atmosphere helps reduce the surface warm bias over the tropical upwelling regions in the coupled models, with further improvements in the cloud cover and precipitation biases particularly over the tropical South Atlantic. Related to this and to the improvement in the precipitation distribution over the western tropical Pacific, the double Intertropical Convergence Zone bias also weakens with resolution. Overall, increased ocean resolution from $\sim 1^\circ$ to
25 $\sim 0.25^\circ$ offers limited improvements or even bias degradation in some models, although an eddy-rich ocean resolution seems beneficial for reducing the biases in North Atlantic temperatures and Gulf Stream path. Despite the improvements, however, large biases in precipitation and cloud cover persist over the whole tropics as well as in the upper-troposphere zonal winds at mid-latitudes in coupled and atmosphere-only models at higher resolutions. The Southern Ocean warm bias also worsens or persists in some coupled models. And a new warm bias emerges in the Labrador Sea in all the high-resolution coupled
30 models. The analysis of the PRIMAVERA models therefore suggests that, to reduce biases, i) increased atmosphere resolution up to $\sim 25\text{--}50$ km alone might not be sufficient and ii) an eddy-rich ocean resolution might be needed. The study thus adds to evidence that further improved model physics and tuning might be necessary in addition to increased resolution to mitigate biases.



1 Introduction

35 Climate models have biases with respect to observations, some of which have persisted over model generations with little or no improvement (e.g., Wang et al., 2014; Tian et al., 2020). These biases can undermine the credibility of climate models, contributing to the uncertainties in regional climate projections (Boberg and Christensen, 2012; Maraun, 2016) and limiting their skill in predicting the climate of coming seasons and decades (e.g., Meehl et al., 2014; Exarchou et al., 2021). Assessing and reducing common model biases are therefore key topics for the climate community to address.

40 Increased model resolution is frequently seen as a way to improve model realism and hence reduce climate biases. Most of the global climate models participating in the CMIP activities have a nominal resolution of about 150 km in the atmosphere and 1° in the ocean (e.g., IPCC, 2013), which ensures a reasonable trade-off between computing-time and model complexity. Higher resolution models have shown important improvements in simulating the Gulf Stream position (e.g., Kirtman et al., 2012; Moreno-Chamarro et al., 2021), the intertropical convergence zone (ITCZ; e.g., Doi et al., 2012; Tian et al., 2020), and
45 the storm tracks (e.g., Hodges et al., 2011), just to mention a few examples. The benefit of higher resolution modelling has extensively been reviewed in Haarsma et al. (2016), Hewitt et al. (2017), or Roberts M.J. et al. (2018).

On this basis, the Horizon2020 [PRIMAVERA](#) project was conceived to “develop a new generation of advanced and well-evaluated high-resolution global climate models, capable of simulating and predicting regional climate with unprecedented fidelity, for the benefit of governments, business and society in general”. Such new models have shown
50 improvements in the representation of various aspects of weather and climate variability, including blocking frequency over the Pacific and Atlantic (Schiemann et al., 2020), the distribution of precipitation over Europe (Demory et al., 2020), tropical cyclones (Roberts M.J. et al., 2020a; Vidale et al., 2021; Zhang et al., 2021), air–sea interactions over the Gulf Stream (Bellucci et al., 2021), and Atlantic ocean heat transports (Roberts M.J. et al., 2020b). In this study, we provide a systematic assessment of the impact of ocean and atmospheric resolution on mean climate (Section 3), with a particular focus on the
55 following long-standing biases: (i) the warm bias in the eastern tropical oceans, (ii) the double ITCZ, (iii) the warm Southern Ocean (SO), and (iv) the cold North Atlantic (Sections 4 and 5). A brief introduction to each bias is provided below in the Introduction. The models, experimental design, and observational data sets are described in Section 2, while the main conclusions and the discussion of the results are in Section 6.

1.1 Biases in the tropics

60 1.1.1 Upwelling regions

The first long-standing bias examined is the warm bias in the eastern tropical oceans, which affects many state-of-the-art and previous-generation climate models (Li and Xie, 2012; Xu et al., 2014a; Richter, 2015; Richter and Tokinaga, 2020). The eastern tropical oceans are characterized by intense coastal upwelling driven by the trade winds, which bring cold, nutrient-rich waters from the deep ocean to the surface and transport them several thousand kilometers offshore. Cold surface
65 waters contrast with warmer atmospheric temperature aloft, which generates stable atmospheric conditions that favors the



formation of large shallow stratocumulus decks. These reflect a large fraction of the solar radiation and thereby help sustain the cold ocean surface below. This system is misrepresented in many climate models, which fail to reproduce the cold tongue of surface waters and hence exhibit a warm bias extending offshore (see, for example, bottom left panel in Fig. 1b). This bias has long been related to the underestimation of the cloud cover, which leads to warming due to excessive shortwave radiation reaching the surface (e.g., Richer, 2015). In turn, the warm bias weakens the lower tropospheric stability and thus hinders the formation of the stratocumulus deck, which contributes to sustaining the surface warm bias. Other mechanisms have been proposed to explain this bias, including too weak alongshore winds weakening the coastal upwelling, too weak offshore transport by ocean mesoscale eddies, and the misrepresentation of the sharp vertical temperature gradient in the upper ocean. All these mechanisms have been reviewed in detail by Richer (2015).

70 Increased horizontal (typically beyond $\sim 25\text{--}50$ km) and vertical resolution in the atmosphere can reduce the warm bias due to improved representation of coast-parallel winds and better-resolved orography, especially along the coast of west Africa (Gent et al., 2010; Milinski et al., 2016; Harlaß et al., 2018). A mesoscale-resolving oceanic resolution can also mitigate the warm bias by improving the representation of the complex coastal current system, as well as the mesoscale eddy contribution to the upper-ocean heat budget and offshore transport from the upwelling regions in the Atlantic (Seo et al., 2006; Xu et al., 2014b; Small et al., 2015). However, the bias persists in some models and ocean basins such as the Pacific even after increasing their resolution (Jochum et al., 2005; Doi et al., 2012; Delworth et al., 2012; Milinski et al., 2016), which suggests that a refinement of model physics might still be necessary to remove it (Patricola et al., 2012; Harlaß et al., 2018). An improvement in the temperature and cloud biases in the eastern tropical oceans can help reduce current uncertainty about climate sensitivity (Andrews et al., 2019) and further enhance models' predictive skill over the tropics (Exarchou et al., 85 2021).

1.1.2 The double ITCZ

Another long-standing bias of the tropical climate in GCMs affects the representation of the ITCZ, referred to as the double ITCZ. This bias takes the form of a tropical precipitation distribution with two distinct maxima, to the north and south of the equator, instead of a single one north of the equator, as in observations (Fig. 2a, and black line in Fig. 3; Schneider et al., 90 2014). The double ITCZ problem has persisted over climate model generations (e.g., Lin, 2007; Li and Xie, 2014; Oueslati and Bellon, 2015; Zhang et al., 2015; Samanta et al., 2019; Tian and Dong, 2020); it has been related to deficiencies in the tropical or global energy budget (Hwang and Frierson, 2013; Bischoff and Schneider, 2016; Adam et al., 2016 & 2018), in atmospheric deep convection (Zhang and Wang, 2006; Oueslati and Bellon, 2015; Song and Zhang, 2019), in land temperature (Zhou and Xie, 2017), and in the atmosphere–ocean coupling due to sea-surface temperature (SST) biases 95 amplified by the wind–evaporation–surface temperature and the Bjerkness feedbacks (Lin, 2007; Li and Xie, 2014; Qin and Lin, 2018; Samanta et al., 2019). The double ITCZ commonly develops together with a cold surface bias and too weak easterlies over the equatorial western Pacific, which lead to reduced convective precipitation aloft (Lin, 2007; Li and Xie, 2014; Oueslati and Bellon, 2015; Zhang et al., 2015; Samanta et al., 2019). The double ITCZ bias can present distinct



seasonal characteristics (Lin, 2007; Li and Xie, 2014; Oueslati and Bellon, 2015; Adam et al., 2018)—although we will
100 focus on the annual mean in our analysis for the sake of simplicity.

Increased model resolution can alleviate the double ITCZ bias, especially over the Atlantic when the eastern tropical warm
bias is reduced (Seo et al., 2006; Delworth et al., 2012; Doi et al., 2012; Harlaß et al., 2018; Song and Zhang, 2020) and
when orography or mesoscale systems are better resolved in models (de Souza Custodio et al., 2017; Vanni re et al., 2019;
105 Monerie et al., 2020). Strong biases in the ITCZ however still develop in high-resolution models (Gent et al., 2010; McClean
et al., 2011; Raj et al., 2019), which might further be reduced through improved convective parametrizations (Zhang et al.,
2019) or the use of atmospheric convection-permitting (i.e., storm-resolving) climate models (Klocke et al., 2017)).

1.2 Biases in middle and high latitudes

In addition to biases in the tropics, climate models also present substantial biases at higher latitudes, which have also
persisted across model generations. Here, we will discuss two of the best-known: the SO surface warm bias, and the cold
110 bias in the subpolar North Atlantic.

1.2.1 Southern Ocean

Both past and state-of-the-art climate models show a surface warm bias over large areas at mid- and higher-latitudes of the
SO (see for example the bottom left panel in Fig. 1b; Schneider and Reusch, 2016; Beadling et al., 2020). This bias has been
attributed to an excessive shortwave radiation reaching and warming the surface ocean as a result of an underestimated cloud
115 cover (especially mixed-phase clouds) and errors in the cloud forcing (Hwang and Frierson, 2013; Bodas-Salcedo et al.,
2012 & 2014; Kay et al., 2016; Schneider and Reusch, 2016; Hyder et al., 2018). The extent and magnitude of these biases
affects important aspects of the climate, not only over the SO but globally. Thus, for example, too warm surface temperatures
result in a gross underestimation of the Antarctic sea ice by models (Beadling et al., 2020). Similarly, the associated
misrepresentation of the low-level temperature gradient has been linked to an equatorward shift bias in the southern
120 hemisphere (SH) upper-troposphere jet (Ceppi et al., 2012). Biases in clouds over the SO are an important uncertainty source
for climate sensitivity (McCoy et al., 2015; Tan et al., 2016). The biggest improvements in the SO warm bias have recently
been achieved through a more realistic representation of cloud properties over the region (Bodas-Salcedo et al., 2014; Seiki
and Roh, 2020; Varma et al., 2020), which might be better characterized in higher resolution models (Furtado and Field,
2017).

1.2.2 The North Atlantic

The bias in the North Atlantic surface temperature is frequently reported in coupled as well as ocean-only climate models,
associated with a misrepresentation of the northward turn of the Gulf Stream (Bryan et al., 2007; IPCC, 2013; Wang et al.,
2014; Marzocchi et al., 2015). The bias is characterized by a warm anomaly off the eastern North American coast, due to a
Gulf Stream separation that is too far north, and a cold anomaly to the east in the central subpolar region, due to a too zonal



130 North Atlantic Current (see, for example, the bottom left panel in Fig. 1b). Improving the representation of the Gulf Stream
and North Atlantic paths, as found in studies using ocean models at eddy-rich resolutions ($\sim 0.1^\circ$ – 0.05° ; Smith et al., 2000;
Bryan et al., 2007; Mertens et al., 2014), may therefore reduce the bias in North Atlantic temperatures (Roberts M.J. et al.,
2019). However, ocean models at relatively high ($\sim 0.25^\circ$ – 0.1°) resolutions can still have substantial biases in subpolar North
Atlantic temperature and salinity compared to 1° or lower resolution models (Delworth et al., 2012; Menary et al., 2015).
135 Instead of increased resolution, ad-hoc corrections to the North Atlantic circulation and surface fluxes can also help alleviate
the North Atlantic bias (Drews et al., 2015). The North Atlantic bias can lead to further biases in the atmospheric circulation
over the entire North Atlantic and Europe (Scaife et al., 2011; Keeley et al., 2012; Lee et al., 2018) and influence the
characteristics of the North Atlantic decadal variability (Menary et al., 2015); an unrealistic Gulf Stream separation can
similarly impact its response to future increases in greenhouse gases (Moreno-Chamarro et al., 2021).

140 2 Experimental setup

2.1 Models and simulations

We compare simulations generated with 5 different climate models participating in the PRIMAVERA project (Table 1):
CNRM-CM6-1 (Voldoire et al., 2019), EC-Earth3P (Haarsma et al., 2020), ECMWF-IFS (Roberts C.D. et al., 2018),
HadGEM3-GC31 (Roberts M.J. et al., 2019), and MPI-ESM1-2 (Gutjahr et al., 2019). Two resolutions for each model are
145 compared (details provided in Table 1): a lower one, which in most cases features a standard ~ 100 – 200 -km atmosphere and
an eddy-none, 1° ocean; and a higher resolution version with a ~ 50 -km atmosphere and an eddy-present, 0.25° ocean. For
simplicity, the lower and higher resolution versions of each model are referred to as LR and HR respectively. In all the
models except for the MPI-ESM1-2 resolution increases in both the ocean and atmosphere from LR to HR (Table 1). For the
MPI-ESM1-2 only the atmosphere resolution increases, from a nominal resolution of 134 km to 67 km, both coupled to a
150 0.4° ocean. To extend the analysis and explore the benefit of an eddy-rich ocean model, we also analyze the HH coupled
version of the HadGEM3-GC31 (Roberts M.J. et al., 2019), which has the same atmospheric resolution as its here-referred
HR version (41 km) but coupled to an eddy-rich, $1/12^\circ$ ocean (Table 1). However, the results of the HadGEM3-GC31-HH
model are simply discussed whenever they are relevant and are not included to compute the ensemble means, since this
model has a different eddy regime compared to the other HR models.
155 Following the CMIP6 HighResMIP protocol, no additional tuning was applied to the HR model versions, except for a short
list of parameters that explicitly change with resolution (especially for oceanic diffusion and viscosity; see, for example,
Table 1 in Roberts M.J. et al., 2020b). Specific details for each model can be found in the references in Table 1. In contrast to
the other models, the HR version of the ECMWF-IFS model was based on an existing configuration used operationally at
ECMWF and then adapted to run at a lower resolution (Roberts C.D. et al., 2018b). We note that four of five coupled models
160 share an ocean component based on NEMO (Nucleus for European Models of the Ocean; Madec et al., 2017):
CNRM-CM6-1, EC-Earth3P, HadGEM3-GC31 use all NEMO v.3.6, and ECMWF-IFS uses NEMO v.3.4, although all differ



in their atmospheric and sea ice components and ocean tuning parameters (more details in the references in Table 1). Similarly, two of five models share an atmosphere component derived from the IFS (Integrated Forecasting System) of the European Centre for Medium-Range Weather Forecasts (ECMWF). Specifically, EC-Earth3P uses IFS cycle 36r4 and
165 ECMWF-IFS uses IFS cycle 43r1. This similarity in the heritage of model configurations might lead to similar biases across the ensemble and thus our results on the impact of resolution may not generalize to all coupled modelling systems.

All simulations follow the HighResMIP experimental design (Haarsma et al., 2016). The experiments consist of i) atmosphere-only simulations (highresSST-present), which are forced by daily, 0.25° SST and sea ice concentration from the Hadley Center Global Ice and Sea Surface Temperature (HadISST.2.2.0; Kennedy et al., 2017), and ii) coupled historical
170 runs (hist-1950), which are forced by time-varying external forcing starting from a 50-year control spin-up that uses fixed 1950s forcing. Both the atmosphere-only and coupled experiments cover the period 1950–2014—although here we focus mainly on the 1980–2014 period (see below). Comparing atmosphere-only and fully coupled climate models might help isolate the biases arising from atmosphere–ocean interactions.

Model simulation output is obtained from the Earth System Grid Federation (ESGF) nodes: CNRM-CM6-1 (Voldoire, 2019a
175 & 2019b), EC-Earth3P (EC-Earth, 2018 & 2019), ECMWF-IFS (Roberts C.D. et al., 2017 & 2018a), HadGEM3-GC31 (Roberts M.J., 2017; Coward and Roberts, 2018; Schiemann et al., 2019), and MPI-ESM1-2 (von Storch et al., 2018a & 2018b).

2.2 Observations and reanalysis

The climate models are compared against a suite of observational and reanalysis products. These include tropospheric
180 temperature and zonal winds from the ERA-Interim reanalysis (Dee et al., 2011), precipitation rate from the version-2 GPCP dataset (Adler et al., 2003), cloud cover from the version-3 ESA Cloud_cci dataset (ESA CCI-CLOUD; Stengel et al., 2020), and net cloud radiative effect computed from the CERES-EBAF dataset (Loeb et al., 2018; Kato et al., 2018). The net cloud radiative effect is computed as the difference between the top-of-the-atmosphere upward net flux and the clear sky component; it represents the net effect of clouds on the radiation budget at the top of the atmosphere, with negative mean
185 values for cloud-induced cooling, and vice versa (Fig. 5a). The periods of comparison between model and observations are adapted to maximize observations' availability until the last simulated year (i.e., 2014). These periods are 1980–2014 for ERA-Interim and GPCP, 1982–2014 for ESA CCI-CLOUD, and 2001–2014 for CERES-EBAF. Biases are computed by adapting the ESMValTool (Eyring et al., 2020) recipe "[recipe_perfmetrics_CMIP5.yml](#)" (Gleckler et al., 2008) to analyse the PRIMAVERA models. The statistical significance of the anomalies between models and observations is calculated based on
190 a two-tailed Student's t-test at the 5 % level.



	CNRM-CM6-1		EC-Earth3P		ECMWF-IFS		HadGEM3-GC31			MPI-ESM-2	
Resolution names	LR	HR	LR	HR	LR	HR	LL ²	HM ²	HH ²	HR	XR
Atmosphere nominal resolution (km) ¹	207	75	107	54	80	40	217	41	41	134	67
Vertical levels (top level)	91 (0.01 hPa)	91 (0.01 hPa)	91 (0.01 hPa)	91 (0.01 hPa)	91 (0.01 hPa)	91 (0.01 hPa)	85 (85 km)	85 (85 km)	85 (85 km)	95 (0.01 hPa)	95 (0.01 hPa)
Ocean resolution (degrees; km)	1° (100)	0.25° (25)	1° (100)	0.25° (25)	1° (100)	0.25° (25)	1° (100)	0.25° (25)	0.08° (8)	0.4° (50)	0.4° (50)
Vertical levels	75	75	75	75	75	75	75	75	75	40	40
References	Voldoire et al. (2019)		Haarsma et al. (2020)		Roberts C.D. et al. (2018b)		Roberts M.J. et al. (2019)			Gutjahr et al. (2019)	

¹ Calculated as the area weighted mean grid box diagonal in Klaver et al. (2020).

² The LL and HH configurations refer to the coupled model versions. The equivalent AMIP resolutions are the LM and HM respectively, with the same low- (L) or high-resolution (H) atmosphere forced by a medium-resolution (M) SST field (Roberts M.J. et al., 2019).

Table 1. Model names, horizontal resolution and vertical levels in the atmosphere and ocean, and reference papers.

3 Global biases

Table 2 summarizes the values of the global root-mean squared deviation (RMSD) and bias of four key variables: near-surface air temperature (SAT), precipitation, cloud cover, and net cloud radiative effect. These variables are chosen to help assess the different regional biases discussed in Sections 4 and 5. On average, the ensemble presents a too cold, wet, and slightly cloudy climate, with excessive radiative cooling from clouds compared to observations. The coupled and atmosphere-only model versions tend to present similar global biases at both resolutions for all variables except for SAT, for which biases are smaller in the atmosphere-only runs—consistent with these being forced by observed SSTs. In terms of RMSD, the ensemble mean presents some of the smallest values, likely as a result of error compensation among members. In contrast to the ensemble mean, the MPI-ESM1-2 models are globally warmer and insufficiently cloudy compared to observations, connected with strong biases over the tropics and subtropics (Figs. S1,S2,S5,S6). The EC-Earth models are the only ones that consistently show a positive radiative forcing bias due to clouds, related to a widespread cloud overestimation



over the SO (Figs. S7,S8). Across the ensemble, the atmosphere-only and coupled CNRM-CM6-1 models show the largest RMSD values particularly in cloud cover and net cloud radiative effect (Table 2), dominated by biases over the tropics and high latitudes (Figs. S5–S8). This contrasts with their relatively low global mean biases, a clear indication of large error compensation between regions. The HadGEM3-GC31 and MPI-ESM1-2 models both have large global mean biases in precipitation (excessively wet) and in cloud cover (respectively, excessively cloudy especially in the tropics, and deficiently cloudy especially in the subtropics and mid-latitudes; Fig. S6); however, these models have the smallest biases in net cloud radiative effect. These results highlight the large differences across models within the ensemble. Compared to previous generation CMIP5 models, the global bias in net cloud radiative effect is generally lower in all the PRIMAVERA coupled models (Table 2; c.f. Table 1 in Calisto et al., 2014).

The increase in resolution from LR to HR has on average a mixed effect on the global biases (Table 2). The temperature and net cloud radiative effect biases are reduced, related to improvements in the eastern tropical oceans (Section 4) and North Atlantic (Section 5) particularly in the coupled versions of the HadGEM3-GC31 and ECMWF-IFS models. By contrast, the precipitation and cloud cover biases worsen with increased resolution, especially the cloud excess in the CNRM-CM6-1 and HadGEM3-GC31 models. In most cases, nonetheless, increased resolution has a small impact on the global biases. Since the study of global biases hides large regional differences, we discuss these in the following sections.

4 Biases in the tropics

4.1 Upwelling regions

In the PRIMAVERA models, only the coupled configurations show a distinct warm bias in the eastern tropical oceans of a magnitude of about 2–3 °C (Fig. 1). This bias is absent in the atmosphere-only models, as these are forced by observed SSTs. At LR, the bias is especially persistent over the eastern tropical South Atlantic and South Pacific and extends from the coast equatorward. In the Northern Hemisphere (NH) the warm bias is less robust across models: off the Californian coast, only the CNRM-CM6-1, EC-Earth3P, and MPI-ESM1-2 models show a distinct warm bias (Fig. S2), whereas off northwest Africa, most models present a cold bias instead—likely the result of the strong cold bias in the subpolar region (discussed in Section 5.2).

Increased resolution leads to a ~1 °C reduction in the bias in SH ocean basins in the ensemble mean (Fig. 1), which might be related to improved coastal wind systems (Small et al., 2015; Milinski et al., 2016). The warm bias is largely reduced in both HadGEM3-GC31 HR models, although using an eddy-rich ocean model (HH) offers no further improvement compared to the eddy-present ocean (HM) for the same ~50-km atmosphere resolution (Fig. S2). Therefore, for this model and bias in particular, the increase in atmosphere resolution from a ~200 km to a ~50 km model seems to be more beneficial than the increase in the ocean from ~100 km to ~8 km (Roberts M.J. et al., 2019).



		SAT (°C)				Precipitation (mm d ⁻¹)				Cloud Cover (%)				Net cloud radiative effect (Wm ⁻²)			
		RMSD		Bias		RMSD		Bias		RMSD		Bias		RMSD		Bias	
		Atm.	Coup.	Atm.	Coup.	Atm.	Coup.	Atm.	Coup.	Atm.	Coup.	Atm.	Coup.	Atm.	Coup.	Atm.	Coup.
Ensemble Mean	LR	0.74	1.14	-0.30	-0.66	0.85	0.97	0.25	0.21	9.42	9.57	0.18	0.46	7.03	7.54	-1.52	-1.68
	HR	0.76	1.13	-0.25	-0.51	0.87	0.93	0.30	0.25	9.02	9.31	0.59	0.86	6.64	6.98	-1.27	-1.27
CNRM-CM6		1.30	1.86	-0.60	-1.11	1.19	1.19	0.27	0.21	13.47	13.53	0.20	-0.44	12.33	12.45	-5.45	-5.09
		1.12	2.08	-0.42	-1.38	1.24	1.20	0.33	0.21	13.74	13.64	3.14	2.71	11.27	11.73	-4.43	-3.95
EC-Earth3P		0.87	1.16	-0.45	0.24	0.76	1.00	0.14	0.17	8.61	9.13	0.55	0.02	8.88	9.48	1.76	2.65
		0.99	1.31	-0.51	-0.15	0.87	0.93	0.21	0.22	7.89	8.34	-0.55	-0.74	8.99	9.35	0.27	1.11
ECMWF-IFS		0.90	2.29	-0.58	-1.39	0.74	1.05	0.19	0.13	7.99	8.96	0.45	1.23	9.34	10.51	-2.85	-3.18
		0.98	1.57	-0.58	-0.28	0.79	0.98	0.26	0.26	7.70	8.55	-1.02	-0.83	8.87	9.33	-2.42	-2.36
HadGEM3-GC31	LR	1.15	1.90	-0.16	-1.22	1.27	1.15	0.41	0.34	12.49	12.50	4.33	5.84	7.66	7.87	-0.97	-1.67
	HR (HM)		1.33		-0.66		1.19		0.38		13.73		8.57		6.97		-0.44
	HR (HH)	0.90		-0.06		1.20		0.46		13.18		7.53		6.83		-0.21	
MPI-ESM1-2		1.15	1.33	0.29	0.17	1.08	1.28	0.23	0.21	11.15	11.26	-4.65	-4.36	8.36	8.51	-0.10	-1.08
		1.27	1.40	0.35	-0.07	1.10	1.26	0.24	0.20	11.93	11.64	-6.17	-5.51	8.02	7.80	0.42	-0.71

Table 2. For the variables shown in Figures 1–5, root-mean-square deviation (RMSD) and mean bias (Bias) in the atmosphere-only (Atm.) and coupled (Coup.) models at LR and HR, including the HadGEM3-GC31-HH coupled model. For each variable, the white-to-yellow shading reflects the RMSD gradient between its minimum (white) and maximum (yellow) values; the red-to-blue shading, which is centered around the zero value, represents the bias values for each variable, blue meaning an excessively cold and wet model with negative biases in the cloud cover and net cloud radiative effect compared to observations (and vice versa).

As in many previous-generation GCMs, the surface warm bias is associated with an underestimation of the cloud cover by 10–20 % over the eastern subtropical ocean in the LR ensemble (Fig. 4). The shape and magnitude of the cloud cover bias are similar in the atmosphere-only and coupled models, which points to deficiencies in the atmosphere model as its root cause. The ensemble mean is largely dominated by the bias in the CNRM-CM6-1 model (of about 20–30 %; Figs. S5,S6);



biases over the upwelling region are, by contrast, nearly half the size in the other models. Although the cloud cover bias persists into HR models in both the atmosphere-only and coupled configurations, it shows an improvement of about 10 %
245 right along the South American western coast. Additionally, increased resolution reduces the cloud cover bias over the eastern South Pacific and Atlantic in the coupled versions of the MPI-ESM1-2 and HadGEM3-GC31 models compared to the improvement in their atmosphere-only versions, which highlight the importance of reducing the surface warm bias underneath and an improved atmosphere–ocean coupling.

The temperature and cloud biases can be connected through the bias in the net cloud radiative effect (Fig. 5), which is
250 positive ($10\text{--}20 \text{ Wm}^{-2}$) along the western coasts of the subtropical South Atlantic and North and South Pacific in the ensemble mean. The bias, which is dominated by the shortwave component (not shown), points to an excessive radiative surface warming linked to cloud cover deficit (Fig. 4). Increased resolution helps reduce the bias in the net cloud radiative effect by $10\text{--}15 \text{ Wm}^{-2}$ in the ensemble mean (Fig. 5). This is largely thanks to the contributions of the HadGEM3-GC31 and MPI-ESM1-2 models, especially in their coupled configuration, and by about 5 Wm^{-2} in the EC-Earth3P and ECMWF-IFS
255 models, as a result of their improvements in the surface warm and cloud cover biases discussed above. Contrasting with the other ensemble member, both the atmosphere-only versions and the HR coupled version of the MPI-ESM1-2 model show a negative bias in the net cloud radiative effect over the upwelling region (Figs. S7, S8) linked to a slight cloud overestimation (Figs. S5, S7).

4.2 The double ITCZ

260 The PRIMAVERA LR models suffer from large biases in tropical precipitation (Fig. 2). These biases are similar in extent and magnitude compared to previous and contemporary models (CMIP3/5/6; c.f. Fig. 2 in Tian and Dong, 2020). On average, the double ITCZ is particularly clear over the Pacific basin in the PRIMAVERA coupled models (Fig. 2), where the bias presents the characteristic pattern with precipitation deficit over the equator and excess on the northern and southern flanks by about $\mp 2 \text{ mm d}^{-1}$ on average respectively. This pattern can be identified in all the LR coupled models, except for
265 CNRM-CM6-1, in which the precipitation excess is predominantly on the southern flank. Associated with the equatorial dry bias, a cold bias of $1\text{--}2 \text{ }^\circ\text{C}$ also affects the LR coupled models in the western and central equatorial Pacific (Fig. 1). In contrast to the Pacific, the precipitation bias over the tropical Atlantic points to a southward shifted ITCZ, with dry and wet biases to the north and south of the equator respectively, while over the Indian Ocean a too wet precipitation bias extends over the western part of the basin and a dry one over the Indian subcontinent (Fig. 2). Such differences between ocean basins
270 suggest that either different mechanisms are responsible for their biases or each basin responds differently to the same large-scale/global bias. Together, these biases lead to a precipitation excess mainly over the SH tropics in the zonal mean in the LR coupled models (Fig. 3). All the areas with precipitation excess tend to show positive bias in cloud cover up to about $10\text{--}20 \%$ (Fig. 4).

In contrast to the coupled LR models, their atmosphere-only configurations show no clear double ITCZ pattern (Figs. 2 and
275 3). In the zonal mean, in fact, the excess in precipitation is relatively constant across all the tropics in the atmosphere-only



models (Fig. 3). This result suggests that the double ITCZ arises from misrepresented atmosphere–ocean coupling, consistent with previous literature pointing to simulated air–sea interactions and SST as key players in its development (Lin 2007; Li and Xie, 2014; Oueslati and Bellon 2015). The LR atmosphere-only models, instead, present excessively wet ($\sim 1.5\text{--}3$ mm d^{-1} ; Fig. 2) and cloudy tropics ($\sim 10\text{--}20$ %; Fig. 3), particularly over the western parts of all the ocean basins. These regions are where the ocean surface temperature tends to be the warmest, pointing to a too strong precipitation response to the imposed SST field. It is interesting to note that despite the different pattern in precipitation biases over the tropics between the atmosphere-only and the coupled models, their cloud biases are very similar (compare top and bottom panels in Fig. 4b, and between Figs. S5 and S6). Areas with precipitation excess do not systematically present positive cloud cover biases, and vice versa. This suggests that, first, errors compensate across cloud levels or types—convective cloud excess might result, for example, in a deficit in low-level, stratiform clouds—and, second, the atmosphere–ocean coupling has a subsidiary impact on the cloud bias, which most likely arise from deficiencies in the atmosphere model.

Increased model resolution improves the tropical precipitation biases in the coupled models (Figs. 2 and 3), reducing the double ITCZ over the western Pacific (especially in the ECMWF-IFS, MPI-ESM1-2, and HadGEM3-GC31 models; Fig. S4) and the southward shifted ITCZ over the Atlantic (especially in the HadGEM3-GC31 model) by about $2\text{--}3$ mm d^{-1} . In both cases, these improvement develop together with a reduction in the Pacific cold bias (of about 1 °C) and in the eastern tropical south Atlantic warm bias, in agreement with previous literature (Xu et al., 2014a; Siongco et al., 2015; Song and Zhang, 2019). By contrast, cloud biases over these regions worsens by about $5\text{--}10$ % with increased resolution in the coupled models (Fig. 4). Yet increased resolution leads to modest improvements in most of the coupled models (overall smaller than the magnitude of the bias itself), which still exhibit important biases in precipitation and cloud cover over the tropical Pacific and Indian oceans (Figs. 2, and 4) and a clear precipitation excess over the SH tropics (Fig. 3).

In the atmosphere-only models, improvements due to resolution in precipitation and clouds in the tropics are mostly negligible in the ensemble mean, and only the HadGEM3-GC31 model shows a slight improvement over the western tropical North Pacific (Figs. 2 and S3). This points to issues with the atmospheric model physics, which remained unchanged between LR and HR (Section 2). Improvements seen in the HR coupled models therefore arise from increased resolution/improvements in the ocean, better represented coupling, or both.

5 Biases in middle and high latitudes

5.1 Southern Ocean

The SO warm bias does not appear in all the PRIMAVERA LR coupled models (Fig. 1). Excessively warm SATs by about $1\text{--}2$ °C are especially persistent throughout the entire SO in the EC-Earth3P and ECMWF-IFS models (Fig. S2), which both use a combination of an IFS model and a NEMO model—albeit in different versions (Section 2). In the CNRM-CM6-1, MPI-ESM1-2, and HadGEM3-GC31 models, by contrast, biases over the SO show a more mixed pattern, with successive regional warm and cold biases that might result from a different spatial distribution in sea ice. Together with the SO warm



bias, the LR coupled ensemble (and especially the CNRM-CM6-1, EC-Earth3P, and ECMWF-IFS models; Fig. S8) shows an underestimation of the mid-latitude cloud cover by about 5–10 % (Fig. 4) and a positive bias in the net cloud radiative effect of about 10–20 Wm^{-2} (Fig. 5), which is dominated by the shortwave component (not shown). By contrast, the MPI-ESM1-2 model shows a comparably smaller ($\sim 5 \text{ Wm}^{-2}$) and less widespread bias in net cloud radiative effect over the SO (Fig. S8), which might explain its smaller surface temperature biases (Fig. S2). The HadGEM3-GC31 model shows instead a positive bias in cloud cover over the SO (Fig. S6; related to a recently introduced mixed-phase cloud parametrization; Bodas-Salcedo et al., 2019) and an overly strong net cloud radiative effect (Fig. S8); these biases contrast with its weak SO warm bias (Fig. S2) and point to some form of compensating errors (potentially due to the air–sea heat fluxes; Hayder et al., 2018; Williams et al., 2017) leading to reasonable surface temperatures. These results agree with previous studies relating the SO warm bias to the underestimation of the albedo of clouds (Bodas-Salcedo et al., 2012 & 2014). Associated with the SO warm bias, the LR coupled models also present a dry bias at mid-latitudes (Fig. 2). Similarly, they exhibit an equatorward shift in the upper-level jet, even in models with a relatively small SO warm bias, with too weak zonal wind between the surface and the tropopause at around 60° S and too strong zonal wind at upper-levels ($\sim 200\text{--}300 \text{ hPa}$) to the equator (Fig. 6), in agreement with previous studies (Ceppi et al., 2012).

Increased resolution has a mixed effect on the SO warm bias and, although it seems to worsen in the ensemble mean (Fig. 1), this varies substantially across models (Fig. S2): the CNRM-CM6-1 model experiences an improvement of a cold bias in the Weddell Sea, which turns slightly warm biased by about $1\text{--}2 \text{ }^\circ\text{C}$; the EC-Earth3P warms along the Antarctic coast and its widespread SO warm bias persists at HR; the ECMWF-IFS model shows a worsening of its temperature bias by about $1\text{--}2 \text{ }^\circ\text{C}$ on average and very strongly in the Weddell Sea by more than $5 \text{ }^\circ\text{C}$; the MPI-ESM1-2 shows a $1\text{--}2 \text{ }^\circ\text{C}$ cooling of its SO, which becomes cold biased, especially around the Antarctic Peninsula; and the HadGEM3-GC31 model shows a reduction of its coastal cold bias, developing instead a more widespread $1\text{--}2 \text{ }^\circ\text{C}$ warm bias—although the cold bias over the Weddell Sea persists in the HadGEM3-GC31 eddy-rich model. In contrast to temperature, biases in cloud cover and net cloud radiative effect remain relatively unchanged between LR and HR (Figs. 4 and 5). Both the CNRM-CM6-1 and MPI-ESM1-2 models show a slight widespread reduction and increase of about 5 % in their cloud cover underestimation over the SO respectively, while the ECMWF-IFS and MPI-ESM1-2 models present a small weakening and strengthening of about 5 Wm^{-2} of their positive bias in net cloud radiative effect respectively (Figs. S5–S8). Given the small improvements in the biases in the cloud cover and net cloud radiative effect with resolution, the change in the temperature bias over the SO might be related to a change in the sensitivity of the HR coupled models to the similar cloud and radiation biases, or to development of further biases, for example, in the sea ice, mixed layer depth, air–sea heat fluxes, or the strength of the Antarctic Circumpolar Current (e.g., Roberts C.D. et al., 2018b). The dry bias over the SO remains unchanged with increased resolution (Fig. 2). In agreement with previous studies, there is no obvious linkage between the magnitude of the SO bias and the double ITCZ bias in the coupled LR and HR models (Hawcroft et al., 2017). Increased resolution deepens the magnitude of the zonal wind bias over the SH in all the models, although it has little impact on the overall pattern (Fig. 6).



As for the atmosphere-only models, temperature biases over most of the SO are negligible both at LR and HR (Fig. 1). Nonetheless, the LR versions of the CNRM-CM6-1, EC-Earth3P, ECMWF-IFS, and MPI-ESM1-2 models show a cold bias of about 2–4 °C off the Antarctic coast that only in the CNRM-CM6-1 is reduced by about 1–2 °C is reduced at HR (Fig. S1); this coastal cold bias might reflect an issue in the response of the lower atmosphere to the imposed sea ice field, perhaps
345 related to assumed ice/snow thickness used in the land-surface scheme to calculate skin temperature over ice. Biases in precipitation, cloud cover, and cloud radiative effect are comparatively similar to those in the coupled models and show negligible improvements with resolution as well (Fig. 2–5). Biases in the SH jet in atmosphere-only models are similar but of small amplitude to those in the coupled models (Fig. 6).

5.2 The North Atlantic

350 All the PRIMAVERA LR coupled models show a cold bias of about 3–4 °C in the central subpolar North Atlantic and a warm one of about 1–2 °C off the North American east coast (Figs. 1, S2). These temperature biases are absent in the atmosphere-only models, which supports the notion that these are the result of the misrepresentation of the Gulf Stream separation and path by the ocean model. The cold bias is especially strong in the ECMWF-IFS model, where anomalies colder than –5 °C cover the large areas of the subpolar North Atlantic and Nordic Seas (Fig. S2); this strong cold bias results
355 from an unrealistically weak Atlantic meridional overturning circulation (AMOC) and related heat transport, potentially related to the lack of re-tuning compared to its HR version (see Section 2 and Roberts C.D. et al., 2018b). The cold bias also extends northward into Arctic latitudes in the CNRM-CM6-1 and HadGEM3-GC31 models, which points to a misrepresentation of the Arctic sea ice in addition to the Gulf Stream path. The cold bias over the subpolar North Atlantic is accompanied by a dry bias of about 0.5–1 mm d⁻¹ (Fig. 2) and, in most cases, by a reduced cloud cover by about 5–10 %
360 (Fig. 4). The cold bias might also be related to the southward shifted jet in the NH in some models (Fig. 6) due to a southward shift in the maximum of the horizontal temperature gradient (not shown); however, the bias in the NH jet might also be related to a southward shift in the ITCZ/Hadley Circulation (especially in the Atlantic basin; Fig. 2) and the associated intensification of the subtropical jet.

Increased model resolution reduces the magnitude of the cold bias by about 2–3 °C in the ensemble mean (Fig. 1) and in all
365 models but the MPI-ESM1-2 model (Fig. S2). Both the MPI-ESM1-2 LR and HR models use the same ocean resolution (0.4°; Table 2) and present too zonal North Atlantic Current (Müller et al., 2018). Especially remarkable are the ECMWF-IFS and HadGEM3-GC31 models, where the cold bias is strongly reduced (Fig. S2). In the ECMWF-IFS model, this results from a much more realistic AMOC heat transport and sea ice extent in the North Atlantic compared to the LR version (Roberts C.D. et al., 2018b). In the HadGEM3-GC31, on the other hand, the bias is reduced thanks to the
370 improvement in the Gulf Stream/North Atlantic path with increased resolution (Roberts M.J. et al., 2019). The increase in ocean resolution from an eddy-present to an eddy-rich model leads to further improvement in the Gulf Stream separation (Moreno-Chamarro et al., 2021) and a reduced warm bias near the coast (Fig. S2; Roberts M.J. et al., 2019).



In all the HR models, the cold bias over the subpolar North Atlantic is replaced by a warm bias of about 2–3 °C in the Labrador Sea (Fig. 1); this bias is likely related to a too strong heat transport by the North Atlantic circulation and a too low sea ice concentration (Roberts M.J. et al., 2020b), which in the NEMO models has been linked to a too strong ocean deep mixing in the Labrador Sea at the 0.25° resolution (Koenigk et al., 2021). The warming of the entire subpolar North Atlantic is in fact one of the most remarkable differences due to increased resolution between LR and HR coupled models.

Other biases over the region also change with increased resolution: the dry bias over the subpolar North Atlantic is reduced (Fig. 2), likely because of the surface warming; the cloud cover bias remains relatively unchanged (Fig. 4); and the bias in the NH upper-troposphere jet deepens in most models (Fig. 6), which might be related to an intensification in eddy momentum transfer to the jet due to resolution (Willison et al., 2013) and/or to the changes in the vertical structure of the temperature bias across models.

6 Discussion and Conclusions

This paper examines whether increased horizontal resolution in five PRIMAVERA models improves four well-known, long-standing climate biases. These biases are the warm eastern tropical regions, the double ITCZ, the warm Southern Ocean (SO), and the cold North Atlantic. The analysis also considers improvements in global biases. We compare atmosphere-only and fully coupled models to separate biases arising from poorly resolved atmosphere and ocean processes alone, or from atmosphere–ocean coupling. In most of the models, the increase in resolution in both the atmosphere and ocean goes from the traditional grid of ~100 km to one of 25–50 km. The analysis is expanded by including an eddy-rich global model at an 1/12° ocean resolution. Models are compared to observations and a reanalysis for the period 1980–2014. All the PRIMAVERA LR coupled models suffer from the above-mentioned biases, as in previous generation and contemporary models (CMIP3/5/6; IPCC, 2013; Wang et al., 2014; Tian and Dong, 2020). Increased resolution alleviates some of their biases, both globally and regionally, yet only in a few models and not consistently. On average (i.e., in the ensemble mean), the warm eastern tropical ocean, the double ITCZ, and the cold North Atlantic improve at higher resolutions, while the SO warm bias worsens or persists in some models, and a new warm bias emerges in the Labrador Sea in all the models as a result of excessive Atlantic ocean heat transport (Roberts M.J. et al., 2020b) and excessive ocean deep mixing in the Labrador Sea in NEMO models at a 0.25° resolution (Koenigk et al., 2021). Despite some improvements, large biases remain at higher resolutions, especially in precipitation and cloud cover over the tropics and the upper-troposphere zonal wind at mid-latitudes, for which the benefit from resolution is rather modest. Our results are generally in line with previous modeling work suggesting improvements in biases due to increased resolution (e.g., Mertens et al., 2014; Harlaß et al., 2018; Monerie et al., 2020) or not at all depending on the model and region (e.g., Delworth et al., 2012; Menary et al., 2015; Raj et al., 2019; Bador et al., 2020). The emergence of a consistent warm bias in the Labrador Sea at a high resolution poses the question of what new other biases might appear as resolution increases and highlights the difficult task of removing all biases in models.



405 Yet the ensemble mean hides some important differences across the PRIMAVERA ensemble. Compared to the LR versions,
the CNRM-CM6-1 HR model shows modest improvements in most of its biases, although it still exhibits some of the largest
biases in precipitation, cloud cover, net cloud radiative effect over the tropics, and zonal wind at SH mid-latitudes among the
ensemble. The EC-Earth3P HR model improves slightly in the upwelling and subpolar North Atlantic regions but still shows
large biases in tropical precipitation and a widespread SO warm bias. The ECMWF-IFS HR model, the one with the finest
410 atmospheric nominal resolution (~40 km; Table 1), shows a big improvement in the North Atlantic cold bias because of a
much more realistic Atlantic ocean heat transport compared to LR, and a modest improvement in the tropical precipitation
and the eastern tropics; however, it also shows a worsening of the SO warm bias and no major changes in its global cloud
cover biases. The HadGEM3-GC31 model improves the most because all its biases except for the warm SO are reduced with
increased resolution. This includes notable gains in the tropical south Atlantic upwelling region, with improved surface
415 temperature, cloud cover, and precipitation over the upwelling region, and in the North Atlantic, with a more realistic Gulf
Stream path. The North Atlantic bias and the Gulf Stream separation improve even further in the HadGEM3-GC31 at an
eddy-rich ocean resolution (1/12°). Finally, the MPI-ESM1-2 HR model improves in all the regions except for the North
Atlantic, where the LR and HR, both with the same ocean resolution, suffer from a similar bias in the Gulf Stream. Its bias,
however, also improves at an eddy-rich ocean resolution (Gutjahr et al., 2019). Overall, our analysis thus finds modest
420 improvements or even bias degradation when the ocean resolution increases from 1° to 0.25°. Reaching an eddy-rich ocean
resolution might therefore be necessary to improve some of the biases, for example, over the eastern tropical oceans and the
North Atlantic, in agreement with previous studies (e.g., Mertens et al., 2014; Xu et al., 2014b).

An increase in atmosphere resolution contributes to reducing the warm bias over the eastern tropical oceans in the
HadGEM3-GC31 and MPI-ESM1-2 coupled models, potentially related to a more realistic coastal wind system (Small et
425 al., 2015; Milinski et al., 2016). The reduction in the surface warm bias, in turn, helps reduce the precipitation and cloud
cover biases over the region. However, the increase in atmosphere resolution alone does not lead to improvements over most
regions in the atmosphere-only models, which still show strong biases in tropical precipitation over the western ocean basins
at HR. The atmosphere-only models also show biases in cloud cover and net cloud radiative effect over the whole tropics and
in the zonal winds at mid-latitudes very similar to those in the coupled models both at LR and HR. Even though we
430 acknowledge that our conclusions might be both model and region dependent, our analysis suggests that to remove model
biases i) a refinement of the atmosphere resolution alone might not always be sufficient, and ii) reaching eddy-rich ocean
resolutions might be needed. The increase in ocean resolution from eddy-parametrized (~100 km) to eddy-permitting (~10
km) allows models to represent the first baroclinic Rossby radius and might therefore help improve the representation of
small-scale dynamical processes and then biases. In contrast, equivalent phenomena in the atmosphere are already well
435 resolved (the first Rossby radius at mid-latitude is about 1000 km, which corresponds with the synoptic scale). Many of the
challenges of reducing atmospheric model biases are related to interactions between dynamics, radiation, and parameterized
(moist) physics (clouds, convection, radiation). These errors are much more difficult to address with increasing resolution as
they are not obviously related to errors in grid-scale dynamics but in model physics (Kay et al., 2016; Varma et al., 2020).



Increased atmospheric resolution, nonetheless, does improve the representation of weather or extremes, as found, for
440 example, for tropical cyclones (Roberts M.J. et al., 2020a; Vidale et al., 2021; Zhang et al., 2021) and blocking frequency
(Schiemann et al., 2020) in PRIMAVERA models as well as in numerical weather prediction systems (e.g., Lean et al.,
2008).

In addition to increased resolution, improvements in model parametrizations and process representations, specific corrections
applied to models, additional tuning, and longer spin-ups might all be essential to help attenuate model biases. Improved
445 cloud physics based on observational constraints, for example, can reduce the SO biases in the net cloud radiative effect by
about 4 Wm^{-2} and in the surface temperature by about $1 \text{ }^{\circ}\text{C}$ (Kay et al., 2016; Varma et al., 2020). Corrections to the North
Atlantic Current flow and North Atlantic surface freshwater budget, on the other hand, can eliminate the cold North Atlantic
bias entirely (Drews et al., 2015). Further model tuning and longer spin-ups are still to explore. No additional tuning was
performed in the PRIMAVERA models with the change in resolution, in agreement with the HighResMIP protocol (Haarsma
450 et al., 2016). The lack of re-tuning seems to have been critical for the ECMWF-IFS model especially, whose HR version was
first developed and tuned and later reduced in resolution but not re-tuned (Section 2 and Roberts C.D. et al., 2018b). This
process resulted in a large degradation of its AMOC, which is unrealistically weak, and North Atlantic cold bias—even
though the LR version shows a weaker SO warm bias than the HR does (Fig. S2). With respect to longer spin-ups, the
PRIMAVERA models also followed the HighResMIP protocol, which recommended a relatively short 50-year spin-up
455 (Haarsma et al., 2016). In the HadGEM3-GC31 LR coupled model, such a spin-up was found insufficient to stabilize its
large-scale circulation and could therefore have contributed to accentuating some of its biases (Roberts M.J. et al., 2019).
Testing the benefit of model re-tuning and longer spin-ups would however be extremely time and resources consuming if
performed following traditional approaches at the highest resolutions. Further bias reduction might be gained by using new
convection-permitting climate models, as computing power increases with every new model generation (Klocke et al., 2017).
460 To summarize, our study finds limited benefit from increased resolution between the traditional $\sim 100 \text{ km}$ models and the ~ 25
 km ones to reduce long-standing biases, based on an ensemble of high-resolution models developed for the PRIMAVERA
project. At this resolution range, increased resolution in both the atmosphere and ocean can to some extent improve biases in
the eastern tropical oceans, ITCZ, and North Atlantic, where further improvements can be gained by using an eddy-rich
ocean model. In addition to increased resolution, we propose that future efforts should also be directed toward improving
465 model physics and developing innovative high-resolution model tuning approaches for these resolutions.

Code and data availability. The model data used in this work are available from ESGF
(<https://esgf-index1.ceda.ac.uk/search/cmip6-ceda/>) via the references provided in Section 2.1. Freely available are data of
ERA-Interim at <https://www.ecmwf.int/en/forecasts/datasets/reanalysis-datasets/era-interim>, GPCP at
<https://psl.noaa.gov/data/gridded/data.gpcp.html>, ESA cloud cover at <https://climate.esa.int/en/projects/cloud/data/>, and
470 CERES-EBAF at <https://ceres.larc.nasa.gov/data/>. Data and scripts to reproduce the figures can be obtained from
<https://doi.org/10.5281/zenodo.5006136>.



Author contribution. E.M.-C. and L.-P.C. analyzed the model output. S.L.T. assisted in the use of ESMValTool. E.M.-C. wrote the manuscript with input from all authors.

Competing interests. The authors declare that they have no conflict of interest.

475 **Acknowledgements.** This research has been supported by the Horizon2020 project PRIMAVERA (H2020 GA 641727) and IS-ENES3 (H2020 GA 824084). E.M.-C. acknowledges funding from the ESA contract CMUG-CCI3-TECHPROP. E.T. has received funding from the European Union's Horizon 2020 research and innovation programme under the Marie Skłodowska-Curie grant agreement No. 748750 (SPFireSD project).

References

- 480 Adam, O., Schneider, T., Brient, F. and Bischoff, T.: Relation of the double-ITCZ bias to the atmospheric energy budget in climate models, *Geophysical Research Letters*, 43(14), 7670–7677, doi:10.1002/2016GL069465, 2016.
- Adam, O., Schneider, T. and Brient, F.: Regional and seasonal variations of the double-ITCZ bias in CMIP5 models, *Climate Dynamics*, 51(1), 101–117, doi:10.1007/s00382-017-3909-1, 2018.
- Adler, R.F., Huffman, G.J., Chang, A., Ferraro, R., Xie, P.P., Janowiak, J., Rudolf, B., Schneider, U., Curtis, S., Bolvin, D.
485 and Gruber, A.: The version-2 global precipitation climatology project (GPCP) monthly precipitation analysis (1979–present), *Journal of Hydrometeorology*, 4(6), 1147–1167, doi:10.1175/1525-7541(2003)004<1147:TVGPCP>2.0.CO;2, 2003.
- Andrews, T., Andrews, M.B., Bodas-Salcedo, A., Jones, G.S., Kuhlbrodt, T., Manners, J., Menary, M.B., Ridley, J., Ringer, M.A., Sellar, A.A. and Senior, C.A.: Forcings, feedbacks, and climate sensitivity in HadGEM3-GC3. 1 and UKESM1,
490 *Journal of Advances in Modeling Earth Systems*, 11(12), 4377–4394, doi:10.1029/2019MS001866, 2019.
- Bador, M., Boé, J., Terray, L., Alexander, L.V., Baker, A., Bellucci, A., Haarsma, R., Koenigk, T., Moine, M.P., Lohmann, K. and Putrasahan, D.A.: Impact of higher spatial atmospheric resolution on precipitation extremes over land in global climate models, *Journal of Geophysical Research: Atmospheres*, 125(13), e2019JD032184, doi:10.1029/2019JD032184, 2020.
- Beadling, R.L., Russell, J.L., Stouffer, R.J., Mazloff, M., Talley, L.D., Goodman, P.J., Sallée, J.B., Hewitt, H.T., Hyder, P.
495 and Pandde, A.: Representation of Southern Ocean properties across coupled model intercomparison project generations: CMIP3 to CMIP6, *Journal of Climate*, 33(15), 6555–6581, doi:10.1175/JCLI-D-19-0970.1, 2020.
- Bellucci, A., Athanasiadis, P.J., Scoccimarro, E., Ruggieri, P., Gualdi, S., Fedele, G., Haarsma, R.J., Garcia-Serrano, J., Castrillo, M., Putrasahan, D. and Sanchez-Gomez, E.: Air-Sea interaction over the Gulf Stream in an ensemble of HighResMIP present climate simulations, *Climate Dynamics*, 1–19, doi:10.1007/s00382-020-05573-z, 2021.



- 500 Bischoff, T. and Schneider, T.: The equatorial energy balance, ITCZ position, and double-ITCZ bifurcations, *Journal of Climate*, 29(8), 2997–3013, doi:10.1175/JCLI-D-15-0328.1, 2016.
- Boberg, F. and Christensen, J.H.: Overestimation of Mediterranean summer temperature projections due to model deficiencies, *Nature Climate Change*, 2(6), 433–436, doi:10.1038/nclimate1454, 2012.
- Bodas-Salcedo, A., Williams, K.D., Field, P.R. and Lock, A.P.: The surface downwelling solar radiation surplus over the
505 Southern Ocean in the Met Office model: The role of midlatitude cyclone clouds, *Journal of Climate*, 25(21), 7467–7486, doi:10.1175/JCLI-D-11-00702.1, 2012.
- Bodas-Salcedo, A., Williams, K.D., Ringer, M.A., Beau, I., Cole, J.N., Dufresne, J.L., Koshiro, T., Stevens, B., Wang, Z. and Yokohata, T.: Origins of the solar radiation biases over the Southern Ocean in CFMIP2 models, *Journal of Climate*, 27(1), 41–56, doi:10.1175/JCLI-D-13-00169.1, 2014.
- 510 Bodas-Salcedo, A., Mulcahy, J.P., Andrews, T., Williams, K.D., Ringer, M.A., Field, P.R. and Elsaesser, G.S.: Strong dependence of atmospheric feedbacks on mixed-phase microphysics and aerosol-cloud interactions in HadGEM3, *Journal of Advances in Modeling Earth Systems*, 11(6), 1735–1758, doi:10.1029/2019MS001688, 2019.
- Bryan, F.O., Hecht, M.W. and Smith, R.D.: Resolution convergence and sensitivity studies with North Atlantic circulation models. Part I: The western boundary current system, *Ocean Modelling*, 16(3-4), 141–159,
515 doi:10.1016/j.ocemod.2006.08.005, 2007.
- Calisto, M., Folini, D., Wild, M., and Bengtsson, L.: Cloud radiative forcing intercomparison between fully coupled CMIP5 models and CERES satellite data, *Ann. Geophys.*, 32, 793–807, doi:10.5194/angeo-32-793-2014, 2014.
- Ceppi, P., Hwang, Y.T., Frierson, D.M. and Hartmann, D.L.: Southern Hemisphere jet latitude biases in CMIP5 models linked to shortwave cloud forcing, *Geophysical Research Letters*, 39(19), L19708, doi:10.1029/2012GL053115, 2012.
- 520 Coward, A., and Roberts, M.: NERC HadGEM3-GC31-HH model output prepared for CMIP6 HighResMIP hist-1950. [data set] (last access: 20 October 2020), Earth System Grid Federation, doi:10.22033/ESGF/CMIP6.6039, 2018.
- de Souza Custodio, M., Da Rocha, R.P., Ambrizzi, T., Vidale, P.L. and Demory, M.E.: Impact of increased horizontal resolution in coupled and atmosphere-only models of the HadGEM1 family upon the climate patterns of South America, *Climate Dynamics*, 48(9-10), 3341–3364, doi:10.1007/s00382-016-3271-8, 2017.
- 525 Dee, D.P., Uppala, S.M., Simmons, A.J., Berrisford, P., Poli, P., Kobayashi, S., Andrae, U., Balmaseda, M.A., Balsamo, G., Bauer, D.P. and Bechtold, P.: The ERA-Interim reanalysis: Configuration and performance of the data assimilation system, *Quarterly Journal of the Royal Meteorological Society*, 137(656), 553–597, doi:10.1002/qj.828, 2011.
- Delworth, T.L., Rosati, A., Anderson, W., Adcroft, A.J., Balaji, V., Benson, R., Dixon, K., Griffies, S.M., Lee, H.C., Pacanowski, R.C. and Vecchi, G.A.: Simulated climate and climate change in the GFDL CM2.5 high-resolution coupled
530 climate model, *Journal of Climate*, 25(8), 2755–2781, doi:10.1175/JCLI-D-11-00316.1, 2012.
- Demory, M.-E., Berthou, S., Fernández, J., Sørland, S. L., Brogli, R., Roberts, M. J., Beyerle, U., Seddon, J., Haarsma, R., Schär, C., Buonomo, E., Christensen, O. B., Ciarlo, J. M., Fealy, R., Nikulin, G., Peano, D., Putrasahan, D., Roberts, C. D., Senan, R., Steger, C., Teichmann, C., and Vautard, R.: European daily precipitation according to EURO-CORDEX regional



- climate models (RCMs) and high-resolution global climate models (GCMs) from the High-Resolution Model
535 Intercomparison Project (HighResMIP), *Geosci. Model Dev.*, 13, 5485–5506, doi:10.5194/gmd-13-5485-2020, 2020.
- Doi, T., Vecchi, G.A., Rosati, A.J. and Delworth, T.L.: Biases in the Atlantic ITCZ in seasonal–interannual variations for a
coarse-and a high-resolution coupled climate model, *Journal of Climate*, 25(16), 5494–5511,
doi:10.1175/JCLI-D-11-00360.1, 2012.
- Drews, A., Greatbatch, R.J., Ding, H., Latif, M. and Park, W.: The use of a flow field correction technique for alleviating the
540 North Atlantic cold bias with application to the Kiel Climate Model, *Ocean Dynamics*, 65(8), 1079–1093,
doi:10.1007/s10236-015-0853-7, 2015.
- EC-Earth Consortium (EC-Earth): EC-Earth-Consortium EC-Earth3P-HR model output prepared for CMIP6 HighResMIP
hist-1950 [data set] (last access: 20 October 2020). Earth System Grid Federation. doi:10.22033/ESGF/CMIP6.4683, 2018.
- EC-Earth Consortium (EC-Earth): EC-Earth-Consortium EC-Earth3P model output prepared for CMIP6 HighResMIP
545 hist-1950 [data set] (last access: 20 October 2020), Earth System Grid Federation, doi:10.22033/ESGF/CMIP6.4682, 2019.
- Exarchou, E., Ortega, P., Rodríguez-Fonseca, B., Losada, T., Polo, I. and Prodhomme, C.: Impact of equatorial Atlantic
variability on ENSO predictive skill, *Nature Communications*, 12(1), 1-8, doi:10.1038/s41467-021-21857-2, 2021.
- Eyring, V., Bock, L., Lauer, A., Righi, M., Schlund, M., Andela, B., Arnone, E., Bellprat, O., Brötz, B., Caron, L.-P.,
Carvalho, N., Cionni, I., Cortesi, N., Crezee, B., Davin, E. L., Davini, P., Debeire, K., de Mora, L., Deser, C., Docquier, D.,
550 Earnshaw, P., Ehbrecht, C., Gier, B. K., Gonzalez-Reviriego, N., Goodman, P., Hagemann, S., Hardiman, S., Hassler, B.,
Hunter, A., Kadow, C., Kindermann, S., Koirala, S., Koldunov, N., Lejeune, Q., Lembo, V., Lovato, T., Lucarini, V.,
Massonnet, F., Müller, B., Pandde, A., Pérez-Zanón, N., Phillips, A., Predoi, V., Russell, J., Sellar, A., Serva, F., Stacke, T.,
Swaminathan, R., Torralba, V., Vegas-Regidor, J., von Hardenberg, J., Weigel, K., and Zimmermann, K.: Earth System
Model Evaluation Tool (ESMValTool) v2.0 – an extended set of large-scale diagnostics for quasi-operational and
555 comprehensive evaluation of Earth system models in CMIP, *Geosci. Model Dev.*, 13, 3383–3438,
doi:10.5194/gmd-13-3383-2020, 2020.
- Furtado, K. and Field, P.: The role of ice microphysics parametrizations in determining the prevalence of supercooled liquid
water in high-resolution simulations of a Southern Ocean midlatitude cyclone, *Journal of the Atmospheric Sciences*, 74(6),
2001–2021, doi:10.1175/JAS-D-16-0165.1, 2017.
- 560 Gent, P.R., Yeager, S.G., Neale, R.B., Levis, S. and Bailey, D.A.: Improvements in a half degree atmosphere/land version of
the CCSM, *Climate Dynamics*, 34(6), 819–833, doi:10.1007/s00382-009-0614-8, 2010.
- Gleckler, P.J., Taylor, K.E. and Doutriaux, C.: Performance metrics for climate models, *Journal of Geophysical Research:
Atmospheres*, 113, D06104, doi:10.1029/2007JD008972, 2008.
- Gutjahr, O., Putrasahan, D., Lohmann, K., Jungclaus, J. H., von Storch, J.-S., Brüggemann, N., Haak, H., and Stössel, A.:
565 Max Planck Institute Earth System Model (MPI-ESM1.2) for the High-Resolution Model Intercomparison Project
(HighResMIP), *Geosci. Model Dev.*, 12, 3241–3281, doi:10.5194/gmd-12-3241-2019, 2019.



- Haarsma, R. J., Roberts, M. J., Vidale, P. L., Senior, C. A., Bellucci, A., Bao, Q., Chang, P., Corti, S., Fučkar, N. S., Guemas, V., von Hardenberg, J., Hazeleger, W., Kodama, C., Koenigk, T., Leung, L. R., Lu, J., Luo, J.-J., Mao, J., Mizielinski, M. S., Mizuta, R., Nobre, P., Satoh, M., Scoccimarro, E., Semmler, T., Small, J., and von Storch, J.-S.: High Resolution Model
570 Intercomparison Project (HighResMIP v1.0) for CMIP6, *Geosci. Model Dev.*, 9, 4185–4208, doi:10.5194/gmd-9-4185-2016, 2016.
- Haarsma, R., Acosta, M., Bakhshi, R., Bretonnière, P.-A., Caron, L.-P., Castrillo, M., Corti, S., Davini, P., Exarchou, E., Fabiano, F., Fladrich, U., Fuentes Franco, R., García-Serrano, J., von Hardenberg, J., Koenigk, T., Levine, X., Meccia, V. L., van Noije, T., van den Oord, G., Palmeiro, F. M., Rodrigo, M., Ruprich-Robert, Y., Le Sager, P., Tourigny, E., Wang, S., van
575 Weele, M., and Wyser, K.: HighResMIP versions of EC-Earth: EC-Earth3P and EC-Earth3P-HR – description, model computational performance and basic validation, *Geosci. Model Dev.*, 13, 3507–3527, doi:10.5194/gmd-13-3507-2020, 2020.
- Harlaß, J., Latif, M. and Park, W.: Alleviating tropical Atlantic sector biases in the Kiel climate model by enhancing horizontal and vertical atmosphere model resolution: climatology and interannual variability, *Climate Dynamics*, 50(7),
580 2605–2635, doi:10.1007/s00382-017-3760-4, 2018.
- Hawcroft, M., Haywood, J.M., Collins, M., Jones, A., Jones, A.C. and Stephens, G.: Southern Ocean albedo, inter-hemispheric energy transports and the double ITCZ: Global impacts of biases in a coupled model, *Climate Dynamics*, 48(7-8), 2279–2295, doi:10.1007/s00382-016-3205-5, 2017.
- Hewitt, H.T., Bell, M.J., Chassignet, E.P., Czaja, A., Ferreira, D., Griffies, S.M., Hyder, P., McClean, J.L., New, A.L. and
585 Roberts, M.J.: Will high-resolution global ocean models benefit coupled predictions on short-range to climate timescales?, *Ocean Modelling*, 120, 120–136, doi:10.1016/j.ocemod.2017.11.002, 2017.
- Hodges, K.I., Lee, R.W. and Bengtsson, L.: A comparison of extratropical cyclones in recent reanalyses ERA-Interim, NASA MERRA, NCEP CFSR, and JRA-25, *Journal of Climate*, 24(18), 4888–4906, doi:10.1175/2011JCLI4097.1, 2011.
- Hyder, P., Edwards, J.M., Allan, R.P., Hewitt, H.T., Bracegirdle, T.J., Gregory, J.M., Wood, R.A., Meijers, A.J., Mulcahy, J.,
590 Field, P. and Furtado, K.: Critical Southern Ocean climate model biases traced to atmospheric model cloud errors, *Nature Communications*, 9(1), 1–17, doi:10.1038/s41467-018-05634-2, 2018.
- Hwang, Y.T. and Frierson, D.M.: Link between the double-Intertropical Convergence Zone problem and cloud biases over the Southern Ocean, *Proceedings of the National Academy of Sciences*, 110(13), 4935–4940, doi:10.1073/pnas.1213302110, 2013.
- 595 IPCC: Climate Change 2013: The Physical Science Basis. Contribution of Working Group I to the Fifth Assessment Report of the Intergovernmental Panel on Climate Change [Stocker, T.F., D. Qin, G.-K. Plattner, M. Tignor, S.K. Allen, J. Boschung, A. Nauels, Y. Xia, V. Bex and P.M. Midgley (eds.)]. Cambridge University Press, Cambridge, United Kingdom and New York, NY, USA, 1535 pp., 2013
- Jochum, M., Murtugudde, R., Ferrari, R. and Malanotte-Rizzoli, P.: The impact of horizontal resolution on the tropical heat
600 budget in an Atlantic Ocean model, *Journal of Climate*, 18(6), 841–851, doi:10.1175/JCLI-3288.1, 2005.



- Kato, S., Rose, F.G., Rutan, D.A., Thorsen, T.J., Loeb, N.G., Doelling, D.R., Huang, X., Smith, W.L., Su, W. and Ham, S.H.: Surface irradiances of edition 4.0 clouds and the earth's radiant energy system (CERES) energy balanced and filled (EBAF) data product, *Journal of Climate*, 31(11), pp.4501–4527, doi:10.1175/JCLI-D-17-0523.1, 2018.
- Kay, J.E., Wall, C., Yettella, V., Medeiros, B., Hannay, C., Caldwell, P. and Bitz, C.: Global climate impacts of fixing the
605 Southern Ocean shortwave radiation bias in the Community Earth System Model (CESM), *Journal of Climate*, 29(12), 4617–4636, doi:10.1175/JCLI-D-15-0358.1, 2016.
- Keeley, S.P.E., Sutton, R.T. and Shaffrey, L.C.: The impact of North Atlantic sea surface temperature errors on the simulation of North Atlantic European region climate, *Quarterly Journal of the Royal Meteorological Society*, 138(668), 1774–1783, doi:10.1002/qj.1912, 2012.
- 610 Kennedy, J., H. Titchner, N. Rayner, and M. Roberts: input4MIPs.MOHC.SSTsAndSeaIce.HighResMIP.MOHC-HadISST-2-2-0-0-0, version 20170505 [data set], Earth System Grid Federation, doi:10.22033/ESGF/input4MIPs.1221, 2017.
- Kirtman, B.P., Bitz, C., Bryan, F., Collins, W., Dennis, J., Hearn, N., Kinter, J.L., Loft, R., Rousset, C., Siqueira, L. and Stan, C.: Impact of ocean model resolution on CCSM climate simulations, *Climate Dynamics*, 39(6), 1303–1328,
615 doi:10.1007/s00382-012-1500-3, 2012.
- Klaver, R., Haarsma, R., Vidale, P.L. and Hazeleger, W.: Effective resolution in high resolution global atmospheric models for climate studies, *Atmospheric Science Letters*, 21(4), e952, doi:10.1002/asl.952, 2020.
- Klocke, D., Brueck, M., Hohenegger, C. and Stevens, B.: Rediscovery of the doldrums in storm-resolving simulations over the tropical Atlantic, *Nature Geoscience*, 10(12), 891–896, doi:10.1038/s41561-017-0005-4, 2017.
- 620 Koenigk, T., Fuentes-Franco, R., Meccia, V.L., Gutjahr, O., Jackson, L.C., New, A.L., Ortega, P., Roberts, C.D., Roberts, M.J., Arsouze, T. and Iovino, D.: Deep mixed ocean volume in the Labrador Sea in HighResMIP models, *Climate Dynamics*, 1–24, doi:10.1007/s00382-021-05785-x, 2021.
- Lean, H.W., Clark, P.A., Dixon, M., Roberts, N.M., Fitch, A., Forbes, R. and Halliwell, C.: Characteristics of high-resolution versions of the Met Office Unified Model for forecasting convection over the United Kingdom. *Monthly Weather Review*,
625 136(9), 3408–3424, doi:10.1175/2008MWR2332.1, 2008.
- Lee, R.W., Woollings, T.J., Hoskins, B.J., Williams, K.D., O'Reilly, C.H. and Masato, G.: Impact of Gulf Stream SST biases on the global atmospheric circulation, *Climate Dynamics*, 51(9), 3369–3387, doi:10.1007/s00382-018-4083-9, 2018.
- Li, G. and Xie, S.P.: Origins of tropical-wide SST biases in CMIP multi-model ensembles, *Geophysical Research Letters*, 39(22), L22703, doi:10.1029/2012GL053777, 2012.
- 630 Li, G. and Xie, S.P.: Tropical biases in CMIP5 multimodel ensemble: The excessive equatorial Pacific cold tongue and double ITCZ problems, *Journal of Climate*, 27(4), 1765–1780, doi:10.1175/JCLI-D-13-00337.1, 2014.
- Lin, J.L.: The double-ITCZ problem in IPCC AR4 coupled GCMs: Ocean–atmosphere feedback analysis, *Journal of Climate*, 20(18), 4497–4525, doi:10.1175/JCLI4272.1, 2007.



- Loeb, N.G., Doelling, D.R., Wang, H., Su, W., Nguyen, C., Corbett, J.G., Liang, L., Mitrescu, C., Rose, F.G. and Kato, S.:
635 Clouds and the earth's radiant energy system (CERES) energy balanced and filled (EBAF) top-of-atmosphere (TOA)
Edition-4.0 data product, *Journal of Climate*, 31(2), 895–918, doi:10.1175/JCLI-D-17-0208.1, 2018.
- Madec, G., Bourdallé-Badie, R., Bouttier, P.-A., Bricaud, C., Bruciaferri, D., Calvert, D., Jérôme Chanut, J. Emanuela
Clementi, E., Andrew Coward, A., Delrosso, D., Ethé, C., Flavoni, S., Graham, T., Harle, J., Iovino, D., Lea, D., Lévy, C.,
Lovato, T., Martin, N., Masson, S., Mocavero, S., Paul, J., Rousset, C., Storkey, D., Storto, A., and Vancoppenolle, M.:
640 NEMO ocean engine (Version v3.6), Notes Du Pôle De Modélisation De L'institut Pierre-simon Laplace (IPSL), Zenodo,
https://doi.org/10.5281/zenodo.1472492, 2017.
- Maraun, D.: Bias correcting climate change simulations-a critical review, *Current Climate Change Reports*, 2(4), 211–220,
doi:10.1007/s40641-016-0050-x, 2016.,
- Marzocchi, A., Hirschi, J.J.M., Holliday, N.P., Cunningham, S.A., Blaker, A.T. and Coward, A.C.: The North Atlantic
645 subpolar circulation in an eddy-resolving global ocean model, *Journal of Marine Systems*, 142, 126–143,
doi:10.1016/j.jmarsys.2014.10.007, 2015.
- McClean, J.L., Bader, D.C., Bryan, F.O., Maltrud, M.E., Dennis, J.M., Mirin, A.A., Jones, P.W., Kim, Y.Y., Ivanova, D.P.,
Vertenstein, M. and Boyle, J.S.: A prototype two-decade fully-coupled fine-resolution CCSM simulation, *Ocean Modelling*,
39(1-2), 10–30, doi:10.1016/j.ocemod.2011.02.011, 2011.
- 650 McCoy, D.T., Hartmann, D.L., Zelinka, M.D., Ceppi, P. and Grosvenor, D.P.: Mixed-phase cloud physics and Southern
Ocean cloud feedback in climate models, *Journal of Geophysical Research: Atmospheres*, 120(18), 9539–9554,
doi:10.1002/2015JD023603, 2015.
- Menary, M.B., Hodson, D.L., Robson, J.I., Sutton, R.T., Wood, R.A. and Hunt, J.A.: Exploring the impact of CMIP5 model
biases on the simulation of North Atlantic decadal variability, *Geophysical Research Letters*, 42(14), 5926–5934,
655 doi:10.1002/2015GL064360, 2015.
- Meehl, G.A., Goddard, L., Boer, G., Burgman, R., Branstator, G., Cassou, C., Corti, S., Danabasoglu, G., Doblas-Reyes, F.,
Hawkins, E. and Karspeck, A.: Decadal climate prediction: an update from the trenches, *Bulletin of the American
Meteorological Society*, 95(2), 243–267, doi:10.1175/BAMS-D-12-00241.1, 2014.
- Mertens, C., Rhein, M., Walter, M., Böning, C.W., Behrens, E., Kieke, D., Steinfeldt, R. and Stöber, U.: Circulation and
660 transports in the Newfoundland Basin, western subpolar North Atlantic, *Journal of Geophysical Research: Oceans*, 119(11),
7772–7793, doi:10.1002/2014JC010019, 2014.
- Milinski, S., Bader, J., Haak, H., Siongco, A.C. and Jungclaus, J.H.: High atmospheric horizontal resolution eliminates the
wind-driven coastal warm bias in the southeastern tropical Atlantic, *Geophysical Research Letters*, 43(19), 10–455,
doi:10.1002/2016GL070530, 2016.
- 665 Monerie, P.-A., Chevuturi, A., Cook, P., Klingaman, N. P., and Holloway, C. E.: Role of atmospheric horizontal resolution in
simulating tropical and subtropical South American precipitation in HadGEM3-GC31, *Geosci. Model Dev.*, 13, 4749–4771,
doi:10.5194/gmd-13-4749-2020, 2020.



- Moreno-Chamarro, E., Caron, L.P., Ortega, P., Tomas, S.L. and Roberts, M.J.: Can we trust CMIP5/6 future projections of European winter precipitation?, *Environmental Research Letters*, 16(5), 054063, doi:10.1088/1748-9326/abf28a, 2021.
- 670 Müller, W.A., Jungclaus, J.H., Mauritsen, T., Baehr, J., Bittner, M., Budich, R., Bunzel, F., Esch, M., Ghosh, R., Haak, H., Ilyina, T., Kleine, T., Kornblueh, L., Li, H., Modali, K., Notz, D., Pohlmann, H., Roeckner, E., Stemmler, I., Tian, F., and Marotzke, J.: A Higher-resolution Version of the Max Planck Institute Earth System Model (MPI-ESM1. 2-HR), *Journal of Advances in Modeling Earth Systems*, 10(7), 1383–1413, doi:10.1029/2017MS001217, 2018.
- Oueslati, B. and Bellon, G.: The double ITCZ bias in CMIP5 models: Interaction between SST, large-scale circulation and
675 precipitation, *Climate Dynamics*, 44(3-4), 585–607, doi:10.1007/s00382-015-2468-6, 2015.
- Patricola, C.M., Li, M., Xu, Z., Chang, P., Saravanan, R. and Hsieh, J.S.: An investigation of tropical Atlantic bias in a high-resolution coupled regional climate model, *Climate Dynamics*, 39(9), 2443–2463, doi:10.1007/s00382-012-1320-5, 2012.
- Qin, Y. and Lin, Y.: Alleviated double ITCZ problem in the NCAR CESM1: A new cloud scheme and the working
680 mechanisms, *Journal of Advances in Modeling Earth Systems*, 10(9), 2318–2332, doi:10.1029/2018MS001343, 2018.
- Raj, J., Bangalath, H.K. and Stenchikov, G.: West African Monsoon: current state and future projections in a high-resolution AGCM, *Climate Dynamics*, 52(11), 6441–6461, doi:10.1007/s00382-018-4522-7, 2019.
- Richter, I.: Climate model biases in the eastern tropical oceans: Causes, impacts and ways forward, *Wiley Interdisciplinary Reviews: Climate Change*, 6(3), 345–358, doi:10.1002/wcc.338, 2015.
- 685 Richter, I. and Tokinaga, H.: An overview of the performance of CMIP6 models in the tropical Atlantic: mean state, variability, and remote impacts, *Climate Dynamics*, 55(9), 2579–2601, doi:10.1007/s00382-020-05409-w, 2020.
- Roberts, C. D., Senan, R., Molteni, F., Boussetta, S., and Keeley, S.: ECMWF ECMWF-IFS-HR model output prepared for CMIP6 HighResMIP hist-1950 [data set] (last access: 20 October 2020), Earth System Grid Federation, doi:10.22033/ESGF/CMIP6.4981, 2017.
- 690 Roberts, C. D., Senan, R., Molteni, F., Boussetta, S., and Keeley, S.: ECMWF ECMWF-IFS-LR model output prepared for CMIP6 HighResMIP hist-1950 [data set] (last access: 20 October 2020), Earth System Grid Federation, doi:10.22033/ESGF/CMIP6.4982, 2018a.
- Roberts, C. D., Senan, R., Molteni, F., Boussetta, S., Mayer, M., and Keeley, S. P. E.: Climate model configurations of the ECMWF Integrated Forecasting System (ECMWF-IFS cycle 43r1) for HighResMIP, *Geosci. Model Dev.*, 11, 3681–3712,
695 doi:10.5194/gmd-11-3681-2018, 2018b.
- Roberts, M.J.: MOHC HadGEM3-GC31-LL model output prepared for CMIP6 HighResMIP hist-1950 [data set] (last access: 20 October 2020), Earth System Grid Federation, doi:10.22033/ESGF/CMIP6.6042, 2017.
- Roberts, M.J., Vidale, P.L., Senior, C., Hewitt, H.T., Bates, C., Berthou, S., Chang, P., Christensen, H.M., Danilov, S., Demory, M.E. and Griffies, S.M.: The benefits of global high resolution for climate simulation: process understanding and
700 the enabling of stakeholder decisions at the regional scale, *Bulletin of the American Meteorological Society*, 99(11), 2341–2359, doi:10.1175/BAMS-D-15-00320.1, 2018.



- Roberts, M. J., Baker, A., Blockley, E. W., Calvert, D., Coward, A., Hewitt, H. T., Jackson, L. C., Kuhlbrodt, T., Mathiot, P., Roberts, C. D., Schiemann, R., Seddon, J., Vanni re, B., and Vidale, P. L.: Description of the resolution hierarchy of the global coupled HadGEM3-GC3.1 model as used in CMIP6 HighResMIP experiments, *Geosci. Model Dev.*, 12, 4999–5028, 705 doi:10.5194/gmd-12-4999-2019, 2019.
- Roberts, M.J., Camp, J., Seddon, J., Vidale, P.L., Hodges, K., Vanniere, B., Mecking, J., Haarsma, R., Bellucci, A., Scoccimarro, E. and Caron, L.P.: Impact of model resolution on tropical cyclone simulation using the HighResMIP–PRIMAVERA multimodel ensemble, *Journal of Climate*, 33(7), 2557–2583, doi:10.1175/JCLI-D-19-0639.1, 2020a.
- 710 Roberts, M.J., Jackson, L.C., Roberts, C.D., Meccia, V., Docquier, D., Koenigk, T., Ortega, P., Moreno-Chamarro, E., Bellucci, A., Coward, A. and Drijfhout, S.: Sensitivity of the Atlantic meridional overturning circulation to model resolution in CMIP6 HighResMIP simulations and implications for future changes, *Journal of Advances in Modeling Earth Systems*, 12(8), e2019MS002014, doi:10.1029/2019MS002014, 2020b.
- Samanta, D., Karnauskas, K.B. and Goodkin, N.F.: Tropical Pacific SST and ITCZ biases in climate models: Double trouble 715 for future rainfall projections?, *Geophysical Research Letters*, 46(4), 2242–2252, doi:10.1029/2018GL081363, 2019.
- Scaife, A.A., Copsey, D., Gordon, C., Harris, C., Hinton, T., Keeley, S., O'Neill, A., Roberts, M. and Williams, K.: Improved Atlantic winter blocking in a climate model, *Geophysical Research Letters*, 38(23), L23703, doi:10.1029/2011GL049573, 2011.
- Schiemann, R., Vidale, P. L., Hatcher, R., and Roberts, M.: NERC HadGEM3-GC31-HM model output prepared for CMIP6 720 HighResMIP hist-1950 [data set] (last access: 20 October 2020), Earth System Grid Federation. doi:10.22033/ESGF/CMIP6.446, 2019.
- Schiemann, R., Athanasiadis, P., Barriopedro, D., Doblas-Reyes, F., Lohmann, K., Roberts, M. J., Sein, D. V., Roberts, C. D., Terray, L., and Vidale, P. L.: Northern Hemisphere blocking simulation in current climate models: evaluating progress from the Climate Model Intercomparison Project Phase 5 to 6 and sensitivity to resolution, *Weather Clim. Dynam.*, 1, 277–292, 725 doi:10.5194/wcd-1-277-2020, 2020.
- Schneider, T., Bischoff, T. and Haug, G.H.: Migrations and dynamics of the intertropical convergence zone, *Nature*, 513(7516), 45–53, doi:10.1038/nature13636, 2014.
- Schneider, D.P. and Reusch, D.B.: Antarctic and Southern Ocean surface temperatures in CMIP5 models in the context of the surface energy budget, *Journal of Climate*, 29(5), 1689–1716, doi:10.1175/JCLI-D-15-0429.1, 2016.
- 730 Seiki, T. and Roh, W.: Improvements in Supercooled Liquid Water Simulations of Low-Level Mixed-Phase Clouds over the Southern Ocean Using a Single-Column Model, *Journal of the Atmospheric Sciences*, 77(11), 3803–3819, doi:10.1175/JAS-D-19-0266.1, 2020.
- Seo, H., Jochum, M., Murtugudde, R. and Miller, A.J.: Effect of ocean mesoscale variability on the mean state of tropical Atlantic climate, *Geophysical Research Letters*, 33(9), L09606, doi:10.1029/2005GL025651, 2006.



- 735 Siongco, A.C., Hohenegger, C. and Stevens, B.: The Atlantic ITCZ bias in CMIP5 models, *Climate Dynamics*, 45(5), 1169–1180, doi:10.1007/s00382-014-2366-3, 2016.
- Small, R.J., Curchitser, E., Hedstrom, K., Kauffman, B. and Large, W.G.: The Benguela upwelling system: Quantifying the sensitivity to resolution and coastal wind representation in a global climate model, *Journal of Climate*, 28(23), 9409–9432, doi:10.1175/JCLI-D-15-0192.1, 2015.
- 740 Smith, R.D., Maltrud, M.E., Bryan, F.O. and Hecht, M.W.: Numerical simulation of the North Atlantic Ocean at 1/10°, *Journal of Physical Oceanography*, 30(7), 1532–1561, doi:10.1175/1520-0485(2000)030<1532:NSOTNA>2.0.CO;2, 2000.
- Song, X. and Zhang, G.J.: Culprit of the eastern Pacific double-ITCZ bias in the NCAR CESM1.2, *Journal of Climate*, 32(19), 6349–6364, doi:10.1175/JCLI-D-18-0580.1, 2019.
- Song, F. and Zhang, G.J.: The Impacts of Horizontal Resolution on the Seasonally Dependent Biases of the Northeastern Pacific ITCZ in Coupled Climate Models, *Journal of Climate*, 33(3), 941–957, doi:10.1175/JCLI-D-19-0399.1, 2020.
- 745 Stengel, M., Stapelberg, S., Sus, O., Finkensieper, S., Würzler, B., Philipp, D., Hollmann, R., Poulsen, C., Christensen, M., and McGarragh, G.: Cloud_cci Advanced Very High Resolution Radiometer post meridiem (AVHRR-PM) dataset version 3: 35-year climatology of global cloud and radiation properties, *Earth Syst. Sci. Data*, 12, 41–60, doi:10.5194/essd-12-41-2020, 2020.
- 750 Tan, I., Storelvmo, T. and Zelinka, M.D.: Observational constraints on mixed-phase clouds imply higher climate sensitivity, *Science*, 352(6282), 224–227, doi:10.1126/science.aad5300, d016.
- Tian, B. and Dong, X.: The double-ITCZ bias in CMIP3, CMIP5, and CMIP6 models based on annual mean precipitation, *Geophysical Research Letters*, 47(8), e2020GL087232, doi:10.1029/2020GL087232, 2020.
- Vannière, B., Demory, M.E., Vidale, P.L., Schiemann, R., Roberts, M.J., Roberts, C.D., Matsueda, M., Terray, L., Koenig, T. and Senan, R.: Multi-model evaluation of the sensitivity of the global energy budget and hydrological cycle to resolution, *Climate Dynamics*, 52(11), 6817–6846, doi:10.1007/s00382-018-4547-y, 2019.
- 755 Varma, V., Morgenstern, O., Field, P., Furtado, K., Williams, J., and Hyder, P.: Improving the Southern Ocean cloud albedo biases in a general circulation model, *Atmos. Chem. Phys.*, 20, 7741–7751, doi:10.5194/acp-20-7741-2020, 2020.
- Vidale, P.L., Hodges, K., Vannière, B., Davini, P., Roberts, M.J., Strommen, K., Weisheimer, A., Plesca, E. and Corti, S.: Impact of stochastic physics and model resolution on the simulation of Tropical Cyclones in climate GCMs, *Journal of Climate*, 34(11), 4315–4341, doi:10.1175/JCLI-D-20-0507.1, 2021.
- 760 Voltaire, A.: CNRM-CERFACS CNRM-CM6-1 model output prepared for CMIP6 HighResMIP hist-1950 [data set] (last access: 20 October 2020), Earth System Grid Federation, doi:10.22033/ESGF/CMIP6.4039, 2019a.
- Voltaire, A.: CNRM-CERFACS CNRM-CM6-1-HR model output prepared for CMIP6 HighResMIP hist-1950 [data set] (last access: 20 October 2020), Earth System Grid Federation, doi:10.22033/ESGF/CMIP6.4040, 2019b.
- 765 Voltaire, A., Saint-Martin, D., Sénési, S., Decharme, B., Alias, A., Chevallier, M., Colin, J., Guérémy, J.F., Michou, M., Moine, M.P. and Nabat, P.: Evaluation of CMIP6 deck experiments with CNRM-CM6-1, *Journal of Advances in Modeling Earth Systems*, 11(7), 2177–2213, doi:10.1029/2019MS001683, 2019.



- von Storch, J.-S., Putrasahan, D., Lohmann, K., Gutjahr, O., Jungclaus, J., Bittner, M., Haak, H., Wieners, K.-H., Giorgetta, M., Reick, C., Esch, M., Gayler, V., de Vrese, P., Raddatz, T., Mauritsen, T., Behrens, J., Brovkin, V., Claussen, M., Crueger, T., Fast, I., Fiedler, S., Hagemann, S., Hohenegger, C., Jahns, T., Kloster, S., Kinne, S., Lasslop, G., Kornblueh, L., Marotzke, J., Matei, D., Meraner, K., Mikolajewicz, U., Modali, K., Müller, W., Nabel, J., Notz, D., Peters, K., Pincus, R., Pohlmann, H., Pongratz, J., Rast, S., Schmidt, H., Schnur, R., Schulzweida, U., Six, K., Stevens, B., Voigt, A., and Roeckner, E.: MPI-M MPI-ESM1.2-HR model output prepared for CMIP6 HighResMIP hist-1950 [data set] (last access: 20 October 2020), Earth System Grid Federation, doi:10.22033/ESGF/CMIP6.6586, 2018a.
- von Storch, J.-S., Putrasahan, D., Lohmann, K., Gutjahr, O., Jungclaus, J., Bittner, M., Haak, H., Wieners, K.-H., Giorgetta, M., Reick, C., Esch, M., Gayler, V., de Vrese, P., Raddatz, T., Mauritsen, T., Behrens, J., Brovkin, V., Claussen, M., Crueger, T., Fast, I., Fiedler, S., Hagemann, S., Hohenegger, C., Jahns, T., Kloster, S., Kinne, S., Lasslop, G., Kornblueh, L., Marotzke, J., Matei, D., Meraner, K., Mikolajewicz, U., Modali, K., Müller, W., Nabel, J., Notz, D., Peters, K., Pincus, R., Pohlmann, H., Pongratz, J., Rast, S., Schmidt, H., Schnur, R., Schulzweida, U., Six, K., Stevens, B., Voigt, A., and Roeckner, E.: MPI-M MPI-ESM1.2-XR model output prepared for CMIP6 HighResMIP hist-1950 [data set] (last access: 20 October 2020), Earth System Grid Federation, doi:10.22033/ESGF/CMIP6.10307, 2018b.
- Wang, C., Zhang, L., Lee, S.K., Wu, L. and Mechoso, C.R.: A global perspective on CMIP5 climate model biases, *Nature Climate Change*, 4(3), 201–205, doi:10.1038/nclimate2118, 2014.
- Williams, K.D., Copsey, D., Blockley, E.W., Bodas-Salcedo, A., Calvert, D., Comer, R., Davis, P., Graham, T., Hewitt, H.T., Hill, R. and Hyder, P.: The Met Office global coupled model 3.0 and 3.1 (GC3.0 and GC3.1) configurations, *Journal of Advances in Modeling Earth Systems*, 10(2), 357–380, doi:10.1002/2017MS001115, 2017.
- Willison, J., Robinson, W.A. and Lackmann, G.M.: The importance of resolving mesoscale latent heating in the North Atlantic storm track, *Journal of the Atmospheric Sciences*, 70(7), 2234–2250, doi:10.1175/JAS-D-12-0226.1, 2013.
- Xu, Z., Chang, P., Richter, I. and Tang, G.: Diagnosing southeast tropical Atlantic SST and ocean circulation biases in the CMIP5 ensemble, *Climate Dynamics*, 43(11), 3123–3145, doi:10.1007/s00382-014-2247-9, 2014a.
- Xu, Z., Li, M., Patricola, C.M. and Chang, P.: Oceanic origin of southeast tropical Atlantic biases, *Climate Dynamics*, 43(11), 2915–2930, doi:10.1007/s00382-013-1901-y, 2014b.
- Zhang, G.J. and Wang, H.: Toward mitigating the double ITCZ problem in NCAR CCSM3, *Geophysical Research Letters*, 33(6), L06709, doi:10.1029/2005GL025229, 2006.
- Zhang, G.J., Song, X. and Wang, Y.: The double ITCZ syndrome in GCMs: A coupled feedback problem among convection, clouds, atmospheric and ocean circulations, *Atmospheric Research*, 229, 255–268, doi:10.1016/j.atmosres.2019.06.023, 2019.
- Zhang, W., Villarini, G., Scoccimarro, E., Roberts, M., Vidale, P.L., Vanniere, B., Caron, L.P., Putrasahan, D., Roberts, C., Senan, R. and Moine, M.P.: Tropical cyclone precipitation in the HighResMIP atmosphere-only experiments of the PRIMAVERA Project, *Climate Dynamics*, 1–21, doi:10.1007/s00382-021-05707-x, 2021.



Zhang, X., Liu, H. and Zhang, M.: Double ITCZ in coupled ocean-atmosphere models: From CMIP3 to CMIP5, *Geophysical Research Letters*, 42(20), 8651–8659, doi:doi.org/10.1002/2015GL065973, 2015.

Zhou, W. and Xie, S.P.: Intermodel spread of the double-ITCZ bias in coupled GCMs tied to land surface temperature in
805 AMIP GCMs, *Geophysical Research Letters*, 44(15), 7975–7984, doi:10.1002/2017GL074377, 2017.

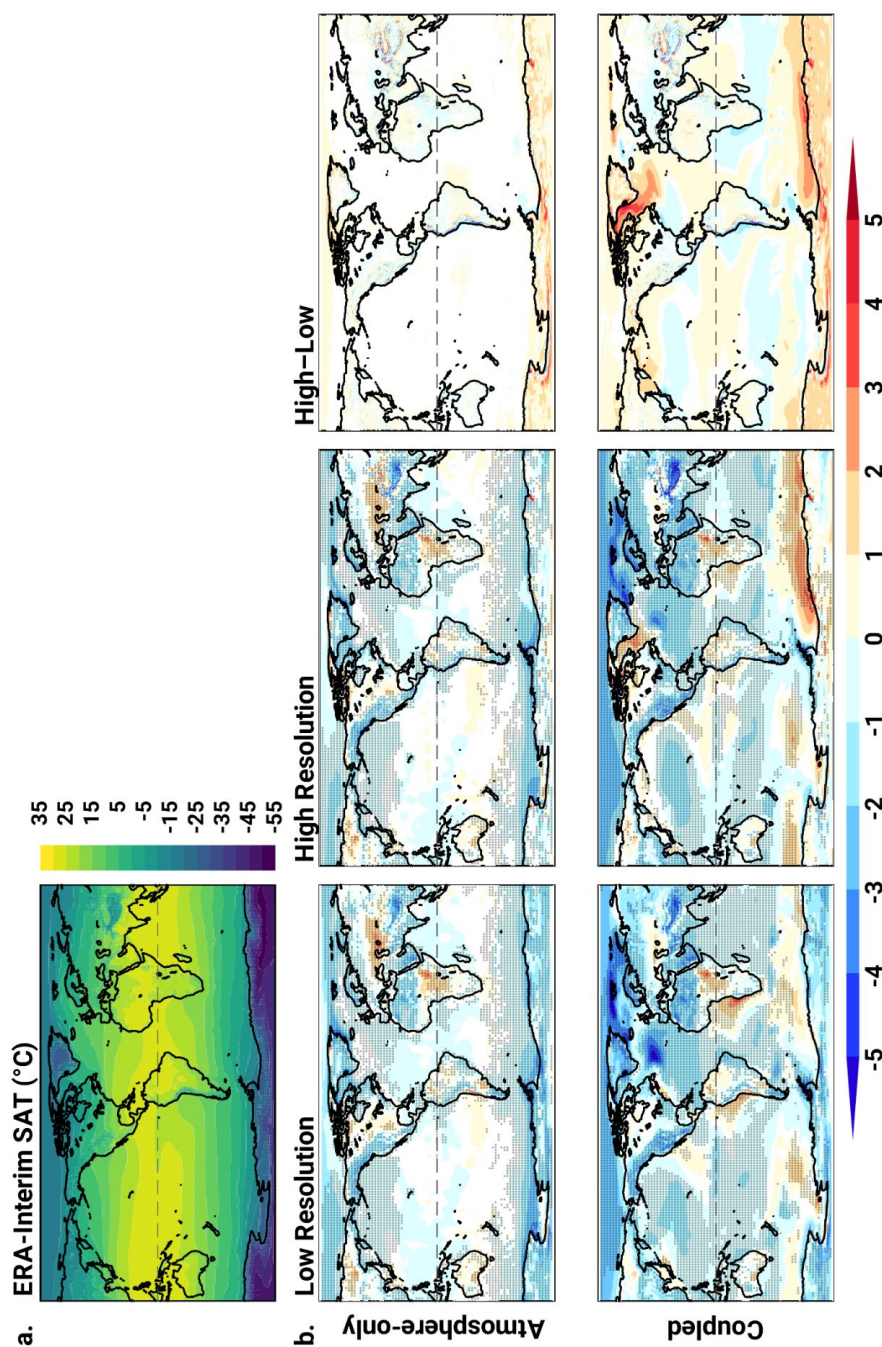


Figure 1. (a) ERA-Interim near-surface (2 m) air temperature (SAT; in °C). (b) *Left and middle:* Multi-model ensemble mean bias in near-surface (2 m) air temperature (in °C) in the atmosphere-only (*top*) and coupled (*bottom*) simulations at low (*left*) and high (*middle*) resolutions. Biases are with respect to ERA-Interim (shown in a.). Stippling masks where at least four out of the five models agree on the anomaly sign. *Right:* Difference between the two resolutions. In all panels non-significant anomalies at the 5 % level (based on a two-tailed Student’s t test) are masked white. The Equator is a dashed line in all the panels.

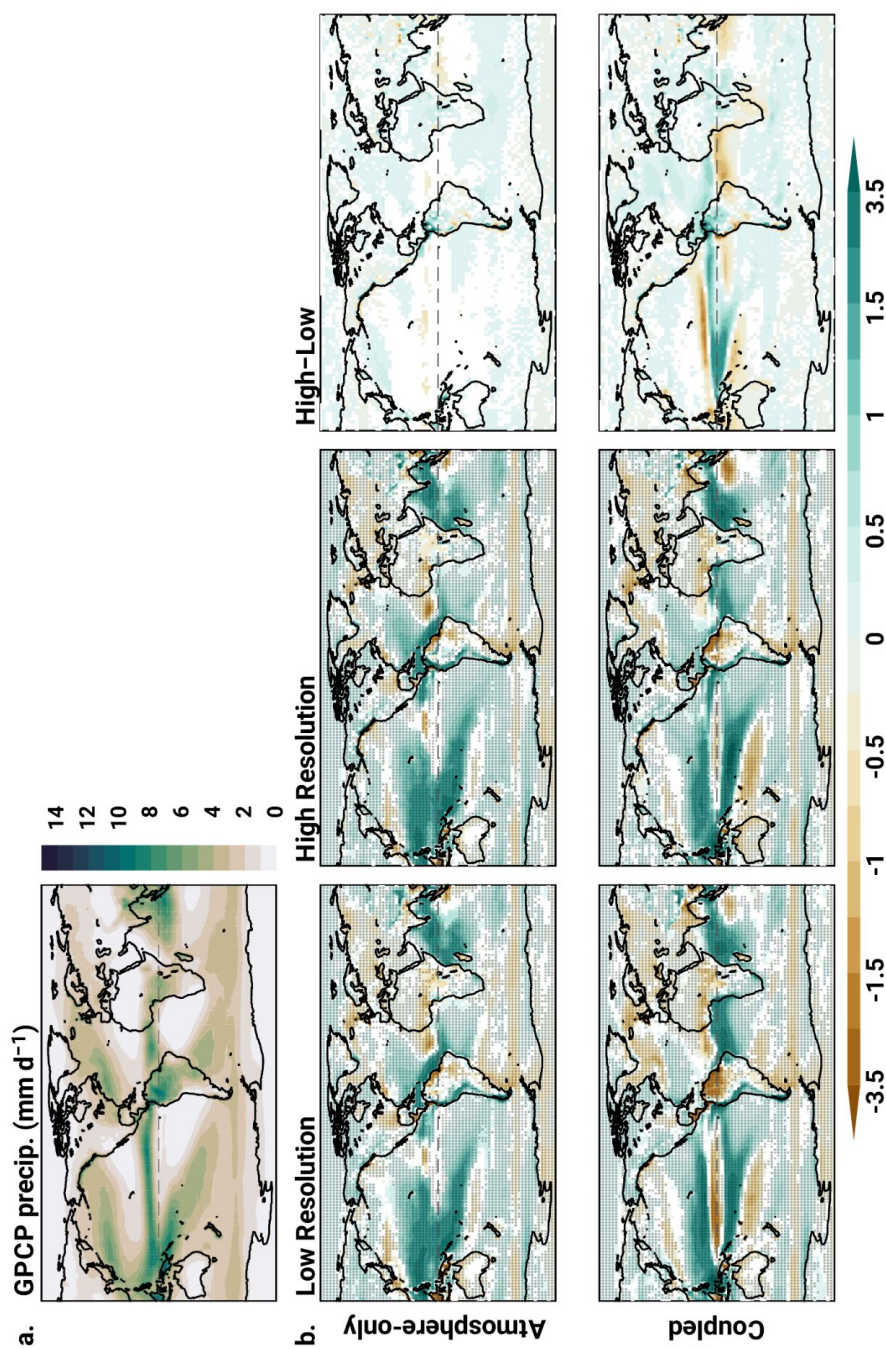


Figure 2. (a) GPCP precipitation rate (in mm d^{-1}). (b) Multi-model ensemble mean bias in precipitation rate (in mm d^{-1}) with respect to the GPCP precipitation at low and high resolution (*left and middle*) and differences between the two resolutions (*right*), as in Fig. 1.

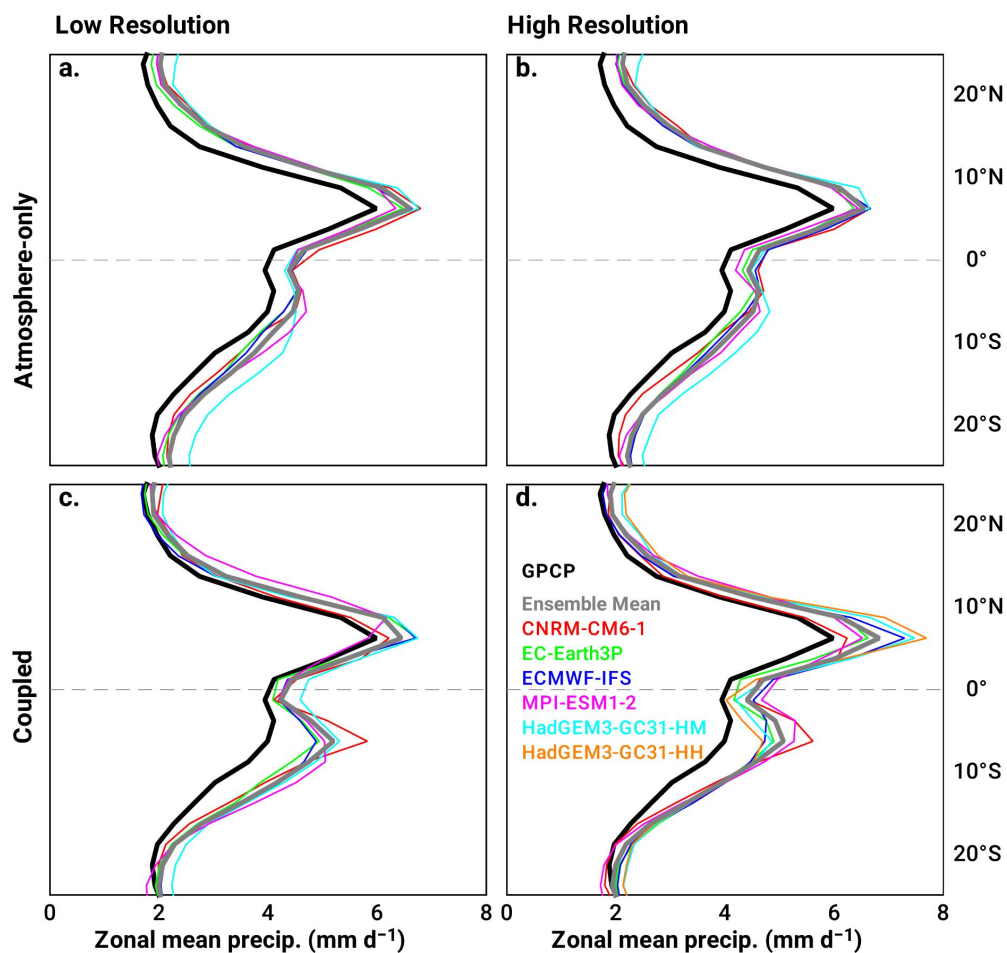


Figure 3. Zonally averaged precipitation rate (in mm d^{-1}) in the tropics for the period 1980–2014 in the atmosphere-only (a,b) and coupled (c,d) models at low (a,c) and high (b,d) resolutions. In all the panels, the individual models are the colored, thin lines, the ensemble mean is the gray, thick line, and the GPCP dataset is the black, thick line. The HadGEM3-GC31-HH (orange line) is shown in d. only.

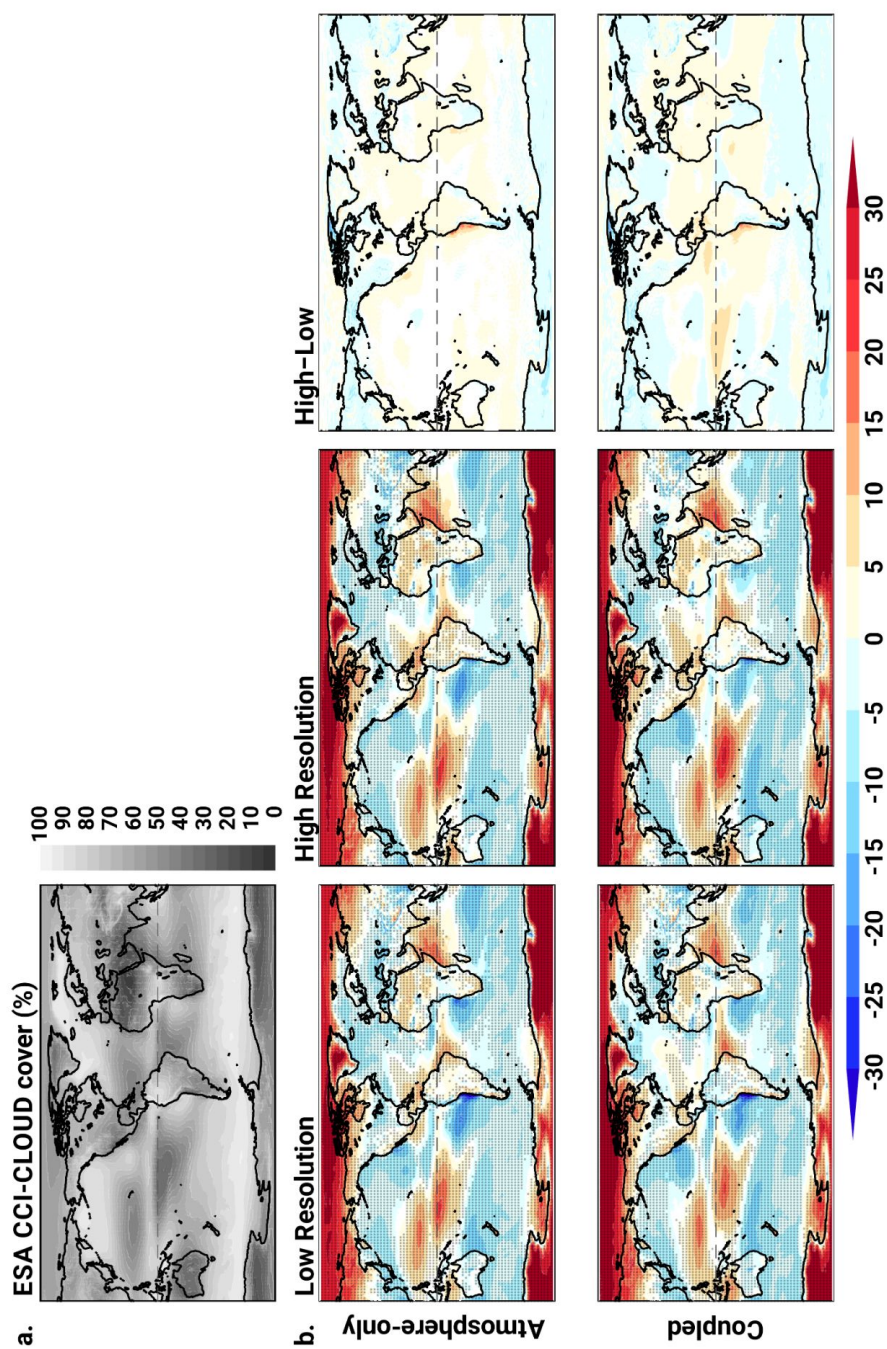


Figure 4. (a) ESA CCI-CLOUD cover (in %). (b) Multi-model ensemble mean bias in net cloud cover (in %) with respect to ESA CCI-CLOUD at low and high resolution (*left and middle*) and differences between the two resolutions (*right*), as in Fig. 1.

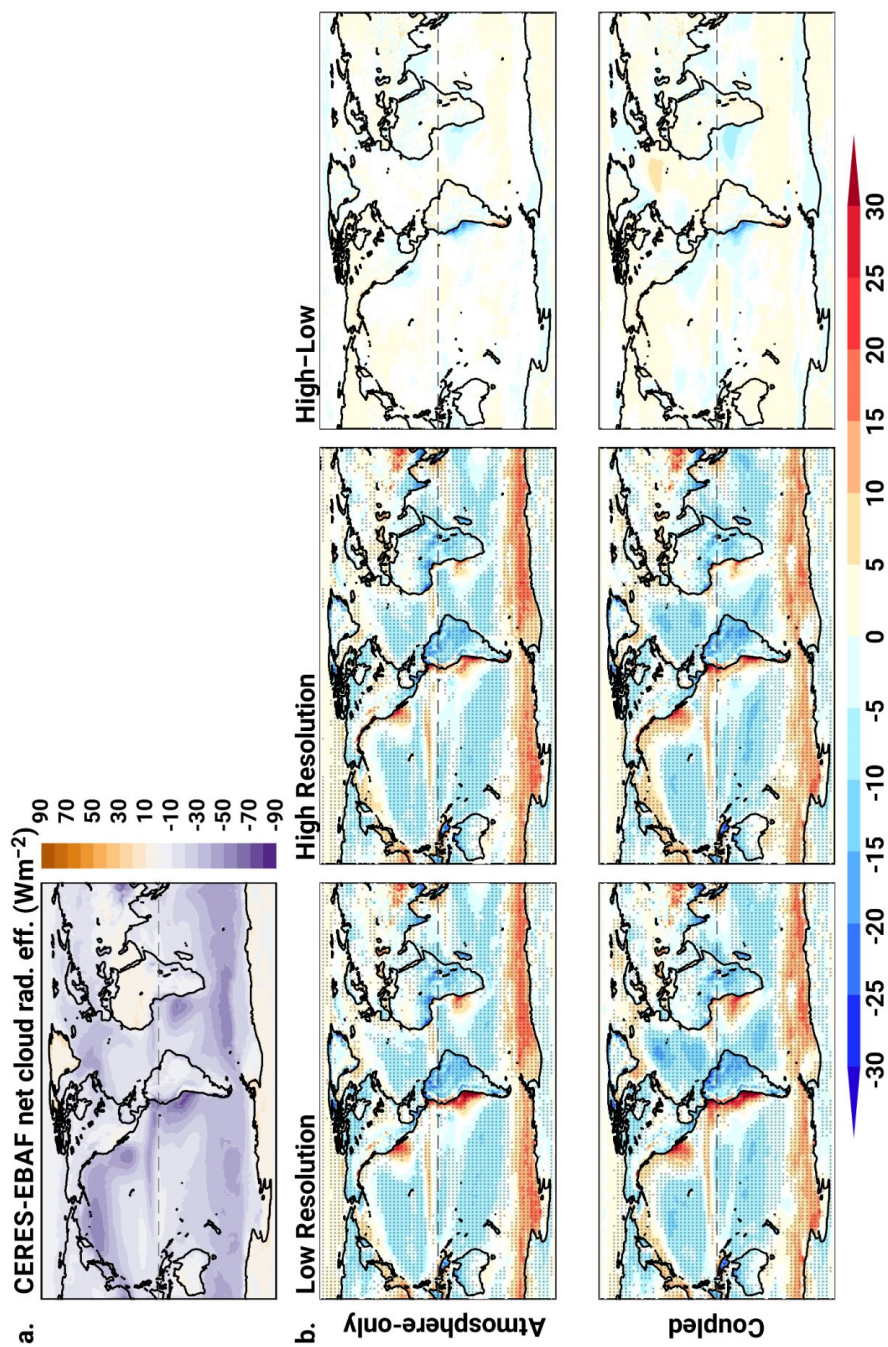


Figure 5. (a) CERES-EBAF net cloud radiative effect (in Wm^{-2}). (b) Multi-model ensemble mean bias in net cloud radiative effect (in Wm^{-2}) with respect to CERES-EBAF at low and high resolution (*left and middle*) and differences between the two resolutions (*right*), as in Fig. 1.

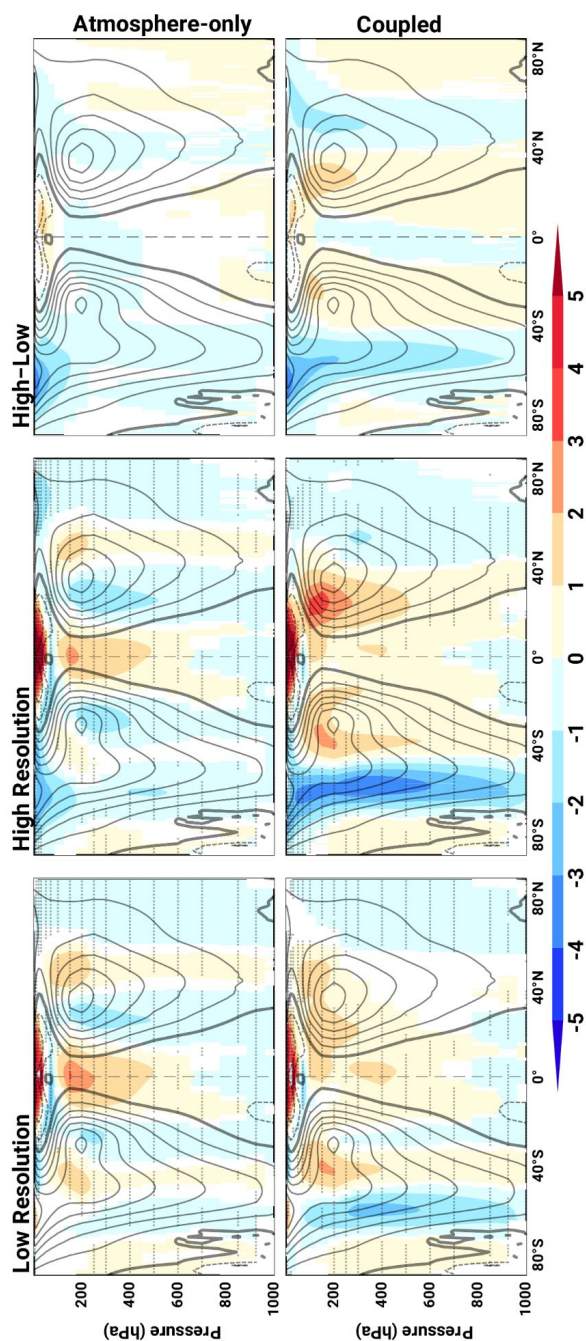


Figure 6. Multi-model ensemble mean bias in the zonally averaged zonal wind (in ms^{-1}) with respect to ERA-Interim at low and high resolution (*left and middle*) and differences between the two resolutions (*right*), as in Fig. 1. Contours represent the ERA-Interim climatology (every 5 ms^{-1} ; negative values, which are for easterlies, are dashed lines, and positive values, for westerlies, are solid lines).